Analysis of Airflow Velocity on Microdroplets Using Weibull Stress-Stress Reliability Index under Unified Type-I Progressive Hybrid Data

Mazen Nassar[1,2], Refah Alotaibi[3] and Ahmed Elshahhat[4,*]

[1] Department of Statistics, Faculty of Science, King Abdulaziz University, Jeddah, 21589, Saudi Arabia

[2] Department of Statistics, Faculty of Commerce, Zagazig University, Zagazig, 44519, Egypt

[3] Department of Mathematical Sciences, College of Science, Princess Nourah bint Abdulrahman University, Riyadh, 11671, Saudi Arabia

[4] Faculty of Technology and Development, Zagazig University, Zagazig, 44519, Egypt

INFORMATION

Keywords:
Stress-strength
microdroplets
weibull
reliability
unified progressive hybrid
Bayesian MCMC-based

DOI: 10.23967/j.rimni.2025.10.69839

SCIPEDIA

Revista Internacional de Métodos Numéricos para Cálculo y Diseño en Ingeniería

RIMNI

Analysis of Airflow Velocity on Microdroplets Using Weibull Stress-Stress Reliability Index under Unified Type-I Progressive Hybrid Data

Mazen Nassar[1,2], **Refah Alotaibi**[3] **and Ahmed Elshahhat**[4,*]

[1]Department of Statistics, Faculty of Science, King Abdulaziz University, Jeddah, 21589, Saudi Arabia

[2]Department of Statistics, Faculty of Commerce, Zagazig University, Zagazig, 44519, Egypt

[3]Department of Mathematical Sciences, College of Science, Princess Nourah bint Abdulrahman University, Riyadh, 11671, Saudi Arabia

[4]Faculty of Technology and Development, Zagazig University, Zagazig, 44519, Egypt

ABSTRACT

This work presents a novel and comprehensive inferential framework for analyzing the stress-strength reliability parameter, $\mathcal{R} = P(Y < X)$, where X and Y denote independent stress and strength variables, respectively, both modeled as Weibull-distributed with a shared shape parameter but distinct scale parameters. A key innovation of this study lies in its integration of the unified Type-I progressively hybrid censoring scheme, which simultaneously accommodates time constraints and partial failure information, conditions often encountered in real-world reliability testing. To estimate R, we propose and evaluate four distinct inferential strategies: two frequentist (maximum likelihood estimation and maximum spacings estimation) and two Bayesian, each tailored to either the likelihood or spacings-based posterior formulation. The Bayesian methods employ Monte Carlo sampling to compute both Bayes point estimates and credible intervals under informative priors, offering robustness in small-sample or heavily censored contexts. An extensive simulation study is conducted to systematically compare the estimators in terms of bias, efficiency, and interval coverage. To validate the practical applicability of our framework, we further analyze two real-world microdroplet datasets, revealing critical insights into stress-tolerance behavior under experimental constraints. This study not only advances methodological tools for reliability inference under hybrid censoring but also establishes a blueprint for combining classical and Bayesian paradigms in stress-strength modeling.

OPEN ACCESS

Received: 01/07/2025

Accepted: 02/09/2025

Published: 23/01/2026

DOI
10.23967/j.rimni.2025.10.69839

Keywords:
Stress-strength
microdroplets
weibull
reliability
unified progressive hybrid
Bayesian MCMC-based

1 Introduction

In statistical reliability analysis, the concept of stress-strength reliability is defined as the probability $\mathcal{R} = P(Y < X)$. This metric quantifies the likelihood that a system's inherent strength, represented by the random variable X, will resist an externally applied stress Y. A system fails when the stress

*Correspondence: Ahmed Elshahhat (aelshahhat@ftd.zu.edu.eg).

surpasses its strength. So, stress-strength reliability gives the chance that the system will keep working under stress, showing how likely it is to avoid failure; for details, see Liu et al. [1] and Cheng et al. [2], among others.

Kotb and Raqab [3] provided many examples of the applications of stress-strength reliability in various fields, not only in engineering but also in physics, medicine, and mechanical systems. The model $\mathcal{R} = P(Y < X)$ was originally introduced by Birnbaum and McCarty [4]. Since that time, many researchers have explored this concept using various probability distributions to model the stress Y and strength X. In addition, estimating the reliability $\mathcal{R} = P(Y < X)$ is a widely studied problem in the statistical literature. Many researchers have explored methods for estimating this probability. For example, Asgharzadeh et al. [5] studied the stress-strength reliability for Weibull distribution using progressively censored sampled. Asgharzadeh et al. [6] considered the estimation for $\mathcal{R} = P(Y < X)$ when X and Y have a generalized logistic distribution. Krishna et al. [7] considered the estimation issues for $\mathcal{R}$ of inverse Weibull distribution using progressively first failure censored samples. Almarashi et al. [8] considered various classical estimations method for $\mathcal{R}$ in the case of Weibull distribution. Kotb and Al Omari [9] studied the stress-strength parameter of the exponential-Rayleigh distribution.

A key step in analyzing the stress-strength model is selecting a suitable statistical distribution to represent both X and Y. Among the many probability distributions available, the Weibull distribution remains one of the most prominent in the statistical literature. It is widely used in reliability and survival analysis due to its flexibility in modeling different types of failure rates—constant, increasing, or decreasing. The Weibull distribution has been widely and effectively used for analyzing lifetime data, especially in situations where the data are censored. In this study, we assume that the random variables X and Y are independent and both follow a Weibull distribution with a common shape parameter but different scale parameters. This assumption simplifies the derivation of the stress-strength reliability parameter and allows for a closed-form estimator in this case. For a detailed overview of the Weibull distribution and its different extensions, see the work by Lai et al. [10]. Suppose that the strength random variable X follows the Weibull distribution with scale parameter $\gamma_1 > 0$ and shape parameter $\phi > 0$, denoted by $W(\gamma_1, \phi)$. In this case, the probability density function (PDF) of X can be expressed as

$$g(x; \gamma_1, \phi) = \gamma_1 \phi x^{\phi-1} e^{-\gamma_1 x^{\phi}}, x > 0. \tag{1}$$

The distribution function corresponding to (1) is

$$G(x; \gamma_1, \phi) = 1 - e^{-\gamma_1 x^{\phi}}. \tag{2}$$

Assuming that the random variables X and Y are independent, where $X \sim W(\gamma_1, \phi)$ and $Y \sim W(\gamma_2, \phi)$, the stress-strength reliability parameter $\mathcal{R} = P(Y < X)$, can be expressed as given by Asgharzadeh et al. [5], as follows

$$\mathcal{R} = \frac{\gamma_1}{\gamma_1 + \gamma_2}. \tag{3}$$

Advancements in engineering, manufacturing, and technology have led to the use of more advanced censoring methods in life-testing studies. This is mainly because it is often difficult for researchers to record the exact failure times for all tested units. The resulting information is called censored data. Pre-planned censoring is commonly used to shorten the duration of an experiment and reduce associated costs. In the statistical literature, numerous censoring methodologies have been proposed, each with its own advantages and distinct stopping rules.

In a life-testing experiment involving n units, let m denote the required number of observed failures and T be a pre-specified termination time. Under the Type-I censoring scheme, the experiment ends at the fixed time T, regardless of how many failures have been observed by that point. In contrast, Type-II censoring terminates the experiment as soon as the m^{th} failure occurs, irrespective of the elapsed time. Epstein [11] introduced the Type-I hybrid censoring (TIHC) method, which stops the test at $min(X_{m:n}, T)$, where $X_{m:n}$ denotes the time of the m^{th} failure. On the other hand, Childs et al. [12] proposed the TIIHC plan, under which the test concludes at $max(X_{m:n}, T)$. For more details about the HC plans, see Balakrishnan and Kundu [13]. Chandrasekar et al. [14] introduced two censoring schemes, namely generalized Type-I HC (GTIHC) and GTIIHC plans, to combine the strengths of both traditional Type-I and Type-II HC plans. These generalized schemes aim to ensure a sufficient number of observed failures while also placing an upper limit on the experimental duration. To explain the GTIHC and GTIIHC schemes, suppose the experimenter specifies, in advance, two integers k and m with $k < m$, along with two time thresholds T_1 and T_2, where $T_1 < T_2$. Under the GTIHC scheme, the test is terminated at $X_{k:n}$ if $X_{k:n} > T_1$, otherwise stop the test at $min(X_{m:n}, T_1)$. On the other hand, in the GTIIHC plan, the test is terminated at T_1 if $X_{m:n} < T_1$. If $T_1 < X_{m:n} < T_2$ the test is concluded at $X_{m:n}$, otherwise the test is stopped at T_2. While the GTIHC and GTIIHC schemes provide enhancements over traditional HC methodologies, they still present some drawbacks. Specifically, the GTIHC scheme does not ensure the observation of a predetermined number of failures, whereas the GTIIHC scheme may result in capturing only a limited number of failure events.

As a result, Balakrishnan et al. [15] proposed a unified hybrid censoring (UHC) plan in which the researcher pre-selects the values of k and m (with $k < m$), along with two threshold times T_1 and T_2 such that $T_1 < T_2$. Based on this scheme, the test is terminated at $\min \max(X_{m:n}, T_1), T_2$ if $T_1 > X_{k:n}$. If $T_1 < X_{k:n} < T_2$, the test ends at $\min(X_{m:n}, T_2)$. Finally, if $X_{k:n} > T_2$, the test is concluded at $X_{k:n}$. The UHC plan has gained considerable popularity due to its adaptability compared to other censoring schemes. This has motivated many researchers to investigate various estimation problems for lifetime distributions under the UHC scheme. See, for example, the works of Panahi and Sayyareh [16], Jeon and Kang [17], and Alotaibi et al. [18]. All the aforementioned censoring schemes are classified as single-stage censoring plans, and they share a common limitation: they do not allow for the removal of test units before the experiment concludes. To enhance the flexibility of the experimental design, Górny and Cramer [19] proposed a unified progressive HC (UPHC) scheme, which integrates the features of both the UHC plan and the progressive Type-II censoring scheme. In their work, they proposed four types of the UPHC schemes, namely unified Type-I, Type-II, Type-III, and Type-IV progressive HC plans. In this study, we focus on the unified Type-I progressive HC (UTIPHC) plan. In the UTIPHC scheme, the experimenter preselects two integers k and m, such that $k < m$, two time thresholds T_1 and T_2 with $T_1 < T_2$, and a progressive censoring scheme $\mathbf{R} = (R_1, \ldots, R_m)$ satisfying $n = m + \sum_{i=1}^{m} R_i$, prior to conducting the experiment.

Similar to the traditional progressive Type-II censoring scheme, when the failure time of the i^{th} unit, denoted by $X_{i:n}$, is observed, the experimenter removes R_i surviving units from the remaining test units. The stopping time of the life-testing experiment under the UTIPHC scheme will be

$$T = max\{min(X_{k:n}, T_2), min(X_{m:n}, T_1)\}.$$

Let d_j represent the number of observed failures recorded before the threshold time T_j for $j = 1, 2$. As outlined by Górny and Cramer [19], the UTIPHC scheme can result in six possible experimental outcomes, as illustrated in Table 1. It is observed from Table 1 that Cases II and III can be combined, as well as Cases IV and V, since the corresponding samples and counter settings are identical. As a result, after combining Cases II and III into Case II, and Cases IV and V into Case III, only four distinct cases need to be considered when analyzing the UTIPHC plan. Based on an observed sample obtained under the UTIPHC scheme, the joint likelihood function (LF) for the various four cases of the observed data can be expressed, ignoring constant term, as

$$L(\boldsymbol{\vartheta};\mathbf{x}) = \prod_{i=1}^{J} g(x_i)[1-G(x_i)]^{R_i}[1-G(T)]^{R^*}, \tag{4}$$

where $\boldsymbol{\vartheta}$ is the vector of unknown parameters, $\mathbf{x}$ denotes the observed UTIPHC sample, x_i corresponds to the i^{th} order statistic $x_{i:n}$, written this way for notational simplicity, J, T and R^* are defined after merging the similar cases, as follows

$$(J,T,R^*) = \begin{cases} \left(m, 0, n-m-\sum_{i=1}^{m-1} R_i\right), & \text{for Case I,} \\ \left(d_1, T_1, n-d_1-\sum_{i=1}^{d_1} R_i\right), & \text{for Case II,} \\ \left(k, 0, n-k-\sum_{i=1}^{k-1} R_i\right), & \text{for Case III,} \\ \left(d_2, T_2, n-d_2-\sum_{i=1}^{d_2} R_i\right), & \text{for Case IV.} \end{cases}$$

Table 1: Various experimental outcomes of the UTIPHC scheme

Case	Ordered values	Sample	Termination point	**R**
I	$X_{k:n} < X_{m:n} < T_1 < T_2$	$X_{1:n}, \ldots, X_{m:n}$	$X_{m:n}$	$R_1, \ldots, R_m$
II	$X_{k:n} < T_1 < X_{m:n} < T_2$	$X_{1:n}, \ldots, X_{d_1:n}$	T_1	$R_1, \ldots, R_{d_1}$
II	$X_{k:n} < T_1 < T_2 < X_{m:n}$	$X_{1:n}, \ldots, X_{d_1:n}$	T_1	$R_1, \ldots, R_{d_1}$
IV	$T_1 < X_{k:n} < X_{m:n} < T_2$	$X_{1:n}, \ldots, X_{k:n}$	$X_{k:n}$	$R_1, \ldots, R_k$
V	$T_1 < X_{k:n} < T_2 < X_{m:n}$	$X_{1:n}, \ldots, X_{k:n}$	$X_{k:n}$	$R_1, \ldots, R_k$
VI	$T_1 < T_2 < X_{k:n} < X_{m:n}$	$X_{1:n}, \ldots, X_{d_2:n}$	T_2	$R_1, \ldots, R_{d_2}$

Recently, some authors considered the UTIPHC scheme in their investigations. For example, Anwar et al. [20] considered the estimations of the stress-strength reliability $\mathcal{R} = P(Y < X)$ of the inverted exponentiated Rayleigh distribution. Lone et al. [21] studied the estimations and the problem of selecting optimal censoring plans for the gamma-mixed Rayleigh distribution. Dutta et al. [22] studied the Kumaraswamy-G family of distributions in the presence of partially observed competing risks data. See also for more details Dutta and Kayal [23] and Bayoud et al. [24].

This study is motivated by several key factors: (1) The broad applicability of the stress-strength reliability model across various fields, and the need to examine it under complex censoring schemes, such as the UTIPHC plan, rather than under complete data or simple censoring types. (2) The Weibull distribution's flexibility in modeling lifetime data, making it suitable for reliability studies. (3) The UTIPHC plan, despite its usefulness, has received limited attention in the literature, likely due to its structural complexity involving four key parameters. (4) Existing research has primarily focused on likelihood-based estimation under the UTIPHC scheme, with little to no attention given to the maximum product of spacings (MPS) method or Bayesian estimation using the spacing function (SF), which in some cases can yield more reliable results than classical approaches. Therefore, the main goal of this study is to estimate the stress-strength reliability parameter $\mathcal{R} = P(Y < X)$ assuming that both stress and strength follow independent Weibull distributions, and the data are collected under the UTIPHC scheme. The main objectives of this research can be outlined as: (1) To derive the maximum likelihood estimator (MLE) and the maximum product of spacings estimator (MPSE) for the stress-strength reliability parameter $\mathcal{R} = P(Y < X)$, along with their corresponding approximate confidence intervals (ACIs). (2) To investigate Bayesian estimation of $\mathcal{R} = P(Y < X)$ using both likelihood-based and spacing-based approaches, including point estimates and credible intervals. (3) To assess the performance of the proposed estimators through extensive simulation studies under different UTIPHC scheme configurations. (4) To demonstrate the practical utility of the methods by applying them to real-life reliability data sets. In this study, we use the squared error loss function to obtain the Bayes estimator of $\mathcal{R}$. This choice can be justified by the importance and wide use of this loss function, although any loss function can be easily used. In addition, the Bayes estimates are obtained numerically through sampling from the posterior distribution using Markov Chain Monte Carlo (MCMC) techniques, as closed-form estimators cannot be derived. In this study, the Bayes estimator of $\mathcal{R} = P(Y < X)$ is derived under the squared error loss function, chosen due to its widespread use and practical relevance. Although alternative loss functions could be applied, the squared error loss offers a straightforward and interpretable criterion. Since closed-form solutions are not available, the Bayes estimates are computed numerically by drawing samples from the posterior distributions using Markov Chain Monte Carlo (MCMC) techniques.

The remainder of this paper is organized as follows: Section 2 presents the derivation of the MLE and ACI for $\mathcal{R}$. Section 3 discusses the MPSE and the associated ACI. Section 4 explores the Bayesian estimates and Bayes credible intervals (BCIs) using both likelihood-based and spacings-based approaches. Section 5 reports the results of a simulation study comparing the accuracy and performance of the various proposed methods. Section 6 presents the analysis of microdroplet datasets to illustrate the applicability of the methods. Finally, Section 7 concludes the paper by highlighting the key findings of the study.

2 Likelihood Estimation

In this section, we study the MLE and ACI of the stress-strength reliability parameter $\mathcal{R} = P(Y < X)$ for the Webull distribution using UTIPHC samples. Let $\mathbf{x}$ be an observed UTIPHC sample taken from a Weibull population with scale parameter γ_1 and shape parameter ϕ, and let $\mathbf{y}$ denote to the observed UTIPHC sample selected from a population that follows the Weibull distribution with scale parameter γ_2 and shape parameter ϕ. In this section, we use the same predefined quantities, n, k, m, T_1, T_2, d_1, and d_2 as described earlier to obtain the observed UTIPHC sample $\mathbf{x}$. Similarly, to generate the observed UTIPHC sample $\mathbf{y}$, we utilize a second set of quantities marked with an asterisk, namely n^*, k^*, m^*, T_1^*, T_2^*, d_1^*, and d_2^* along with the progressive censoring scheme $\mathbf{S} = (S_1, \ldots, S_{m^*})$. In this case, the joint LF of $\boldsymbol{\vartheta} = (\gamma_1, \gamma_2, \phi)^\top$ can be expressed as

$$L(\boldsymbol{\vartheta}; \mathbf{x}, \mathbf{y}) = \left\{ \prod_{i=1}^{J} g(x_i)[1 - G(x_i)]^{R_i}[1 - G(T)]^{R^*} \right\} \left\{ \prod_{i=1}^{D} g(y_i)[1 - G(y_i)]^{S_i}[1 - G(T^*)]^{S^*} \right\}, \tag{5}$$

where

$$(D, T^*, S^*) = \begin{cases} \left(m^*, 0, n^* - m^* - \sum_{i=1}^{m^*-1} S_i\right), & \text{for Case I}, \\ \left(d_1^*, T_1^*, n^* - d_1^* - \sum_{i=1}^{d_1^*} S_i\right), & \text{for Case II}, \\ \left(k^*, 0, n^* - k^* - \sum_{i=1}^{k^*-1} S_i\right), & \text{for Case III}, \\ \left(d_2^*, T_2^*, n^* - d_2^* - \sum_{i=1}^{d_2^*} S_i\right), & \text{for Case IV} \end{cases}.$$

Then, based on the PDF in (1), the CDF in (2) and the LF in (6), we can write the LF of $\boldsymbol{\vartheta}$ as

$$L(\boldsymbol{\vartheta}; \mathbf{x}, \mathbf{y}) = \gamma_1^J \gamma_2^D \phi^{J+D} \exp\left\{\phi H - \gamma_1 \eta(\mathbf{x}; \phi) - \gamma_2 \zeta(\mathbf{y}; \phi)\right\}, \tag{6}$$

where
$H = \sum_{i=1}^{J} \log(x_i) + \sum_{i=1}^{D} \log(y_i)$, $\eta(\mathbf{x}; \phi) = \sum_{i=1}^{J}(1+R_i)x_i^\phi + R^* T^\phi$, and $\zeta(\mathbf{y}; \phi) = \sum_{i=1}^{D}(1+S_i)y_i^\phi + S^* T^{*\phi}$.

The log-LF of (6) follows

$$l(\boldsymbol{\vartheta}; \mathbf{x}, \mathbf{y}) = J\log(\gamma_1) + D\log(\gamma_2) + (J + D)\log(\phi)\phi H - \gamma_1 \eta(\mathbf{x}; \phi) - \gamma_2 \zeta(\mathbf{y}; \phi). \tag{7}$$

By differentiating the objective function in (7) with respect to each parameter γ_1, γ_2, and ϕ, we obtain a system of normal equations. These equations can be solved simultaneously to compute the MLEs, denoted by $\hat{\boldsymbol{\vartheta}} = (\hat{\gamma}_1, \hat{\gamma}_2, \hat{\phi})^\top$. The normal equations are as follows

$$\frac{\partial l(\boldsymbol{\vartheta}; \mathbf{x}, \mathbf{y})}{\partial \gamma_1} = \frac{J}{\gamma_1} - \eta(\mathbf{x}; \phi) = 0, \quad \frac{\partial l(\boldsymbol{\vartheta}; \mathbf{x}, \mathbf{y})}{\partial \gamma_2} = \frac{D}{\gamma_2} - \zeta(\mathbf{y}; \phi) = 0 \tag{8}$$

and

$$\frac{\partial l(\boldsymbol{\vartheta}; \mathbf{x}, \mathbf{y})}{\partial \phi} = \frac{J + D}{\phi} + H - \gamma_1 \eta_1(\mathbf{x}; \phi) - \gamma_2 \zeta_1(\mathbf{y}; \phi) = 0, \tag{9}$$

where $\eta_1(\mathbf{x}; \phi) = \sum_{i=1}^{J}(1 + R_i)x_i^\phi \log(x_i) + R^* T^\phi \log(T)$, and $\zeta_1(\mathbf{y}; \phi) = \sum_{i=1}^{D}(1 + S_i)y_i^\phi \log(y_i) + S^* T^{*\phi} \log(T^*)$.

Using the first two normal equations, we can derive closed-form expressions for the MLEs of γ_1 and γ_2 as functions of the unknown shape parameter ϕ, as follows

$$\hat{\gamma}_1(\phi) = \frac{J}{\eta(\mathbf{x}; \phi)}, \quad \text{and} \quad \hat{\gamma}_2(\phi) = \frac{D}{\zeta(\mathbf{y}; \phi)}. \tag{10}$$

It is clear from (10) that the MLEs $\hat{\gamma}_1$ and $\hat{\gamma}_2$ can be directly computed once the MLE $\hat{\phi}$ is known. To obtain $\hat{\phi}$, we substitute γ_1 and γ_2 with their respective MLEs in the normal equation given in (12). The value of $\hat{\phi}$ is then obtained iteratively as the solution to the fixed-point equation $w(\phi) = \phi$, where

$$w(\phi) = \left[\frac{J\eta^*(\mathbf{x}; \phi) + D\zeta^*(\mathbf{y}; \phi) - H}{J + D}\right]^{-1}, \tag{11}$$

where $\eta^*(\mathbf{x};\phi) = \dfrac{\eta_1(\mathbf{x};\phi)}{\eta(\mathbf{x};\phi)}$ and $\zeta^*(\mathbf{y};\phi) = \dfrac{\zeta_1(\mathbf{y};\phi)}{\zeta(\mathbf{y};\phi)}$. The equation in (11) can be solved using an iterative approach defined by the update rule $w(\phi^{(j)}) = \phi^{(j+1)}$, where $\phi^{(j)}$ denotes the value at the j^{th} iteration. After obtaining the MLE $\hat{\phi}$, the MLEs of γ_1 and γ_2 can be calculated using (10) as $\hat{\gamma}_1 = \hat{\gamma}_1(\hat{\phi})$ and $\hat{\gamma}_2 = \hat{\gamma}_2(\hat{\phi})$. Accordingly, the MLE of the stress-strength reliability parameter $\mathcal{R} = P(Y < X)$ can be obtained using the invariance property of the MLEs as follows

$$\widehat{\mathcal{R}} = \frac{J\zeta(\mathbf{y};\hat{\phi})}{D\eta(\mathbf{x};\hat{\phi}) + J\zeta(\mathbf{y};\hat{\phi})}.$$

The ACI for the stress-strength reliability parameter $\mathcal{R} = P(Y < X)$ can be constructed using the asymptotic properties of its MLE $\widehat{\mathcal{R}}$. To do so, it is necessary to estimate the variance of $\widehat{\mathcal{R}}$. As outlined by [5], this variance can be approximated using the delta method. This technique requires the variance-covariance matrix of the model's parameters. Since deriving the Fisher information matrix analytically can be challenging, we approximate the variance-covariance matrix by inverting the observed Fisher information matrix, as shown below

$$\mathbf{\Sigma}(\hat{\boldsymbol{\vartheta}}) = \begin{bmatrix} -l_{11} & 0 & -l_{13} \\ & -l_{22} & -l_{23} \\ & & -l_{33} \end{bmatrix}^{-1} = \begin{bmatrix} \hat{V}_{11} & 0 & \hat{V}_{13} \\ & \hat{V}_{22} & \hat{V}_{23} \\ & & \hat{V}_{33} \end{bmatrix},$$

where

$$l_{11} = -\frac{J}{\gamma_1^2}, \quad l_{22} = -\frac{D}{\gamma_2^2}, \quad l_{13} = \eta_1(\mathbf{x};\phi), \quad l_{23} = \zeta_1(\mathbf{y};\phi),$$

and

$$l_{33} = -\frac{J+D}{\phi^2} - \gamma_1\eta_2(\mathbf{x};\phi) - \gamma_2\zeta_2(\mathbf{y};\phi), \tag{12}$$

where all the above elements are evaluated at the MLEs of the model parameter, $\eta_2(\mathbf{x};\phi) = \sum_{i=1}^{J}(1 + R_i)x_i^{\phi}\log^2(x_i) + R^*T^{\phi}\log^2(T)$, and $\zeta_2(\mathbf{y};\phi) = \sum_{i=1}^{D}(1 + S_i)y_i^{\phi}\log^2(y_i) + S^*T^{*\phi}\log^2(T^*)$.

By applying the delta method, we can approximate the variance of the MLE of $\mathcal{R} = b(\boldsymbol{\vartheta})$ as

$$\widehat{V}_{\mathcal{R}} \approx \Delta^{\top}\mathbf{\Sigma}(\hat{\boldsymbol{\vartheta}})\Delta, \tag{13}$$

where

$$\Delta^{\top} = \left(\frac{\partial b(\boldsymbol{\vartheta})}{\partial\gamma_1}, \frac{\partial b(\boldsymbol{\vartheta})}{\partial\gamma_2}, \frac{\partial b(\boldsymbol{\vartheta})}{\partial\phi}\right)$$

is the gradient vector of $b(\boldsymbol{\vartheta})$ evaluated at the MLEs of the unknown parameters and given by $\Delta^{\top} = \left(\hat{\gamma}_2, -\hat{\gamma}_1, 0\right)/(\hat{\gamma}_1 + \hat{\gamma}_2)^2$. As a result, we can write $\widehat{V}_{\mathcal{R}}$ in (13) after some simplifications as

$$\widehat{V}_{\mathcal{R}} \approx \frac{\hat{\gamma}_2^2\hat{V}_{11} + \hat{\gamma}_1^2\hat{V}_{22}}{(\hat{\gamma}_1 + \hat{\gamma}_2)^2}.$$

Accordingly, for a given significance level α, the $100\%(1-\alpha)$ ACI of $\mathcal{R}$ can be constructed as

$$\left(\frac{\hat{\gamma}_1 - z_{\alpha/2}\sqrt{\hat{\gamma}_2^2\hat{V}_{11} + \hat{\gamma}_1^2\hat{V}_{22}}}{\hat{\gamma}_1 + \hat{\gamma}_2}, \frac{\hat{\gamma}_1 + z_{\alpha/2}\sqrt{\hat{\gamma}_2^2\hat{V}_{11} + \hat{\gamma}_1^2\hat{V}_{22}}}{\hat{\gamma}_1 + \hat{\gamma}_2}\right),$$

where $z_{\alpha/2}$ represents the critical value from the standard normal distribution $N(0,1)$ that corresponds to the upper $\dfrac{\alpha}{2}$ percentile.

3 Product of Spacings Estimation

In this section, we aim to derive the MPSE and its corresponding ACI for the stress-strength reliability parameter $\mathcal{R}$. In recent years, the MPS method has attracted increased attention due to its desirable properties, which are similar to those of the likelihood method. In some cases, particularly with small samples, which are common in censored data, the MPS method can yield more accurate and stable estimates. This estimation technique was independently proposed by Cheng and Amin [25] and Ranneby [26]. Some recent works on the MPS estimation method include studies by Kateri nd Nikolov [27] and Nassar et al. [28]. Using the two observed UTIPHC samples $\mathbf{x}$ and $\mathbf{y}$, the MPSEs are obtained by maximizing the following product of SF, without constant terms,

$$P(\boldsymbol{\vartheta};\mathbf{x},\mathbf{y}) = \left\{\prod_{i=1}^{J+1}[G(x_i)-G(x_{i-1})]\prod_{i=1}^{J}[1-G(x_i)]^{R_i}[1-G(T)]^{R^*}\right\}$$
$$\times\left\{\prod_{i=1}^{D+1}[G(y_i)-G(y_i)]\prod_{i=1}^{D}[1-G(y_i)]^{S_i}[1-G(T^*)]^{S^*}\right\}. \tag{14}$$

Let $a_i = x_i^{\phi} - x_{i-1}^{\phi}$ and $c_i = y_i^{\phi} - y_{i-1}^{\phi}$, then it follows from the CDF given by (2) and the SF in (14), after some simplifications, that

$$P(\boldsymbol{\vartheta};\mathbf{x},\mathbf{y}) = \exp\left\{\sum_{i=1}^{J+1}\log\left(e^{\gamma_1 a_i}-1\right)+\sum_{i=1}^{D+1}\log\left(e^{\gamma_2 c_i}-1\right)-\gamma_1\eta(\mathbf{x};\phi)-\gamma_2\zeta(\mathbf{y};\phi)\right\}. \tag{15}$$

The log-SF can be expressed as

$$p(\boldsymbol{\vartheta};\mathbf{x},\mathbf{y}) = \sum_{i=1}^{J+1}\log\left(e^{\gamma_1 a_i}-1\right)+\sum_{i=1}^{D+1}\log\left(e^{\gamma_2 c_i}-1\right)-\gamma_1\eta(\mathbf{x};\phi)-\gamma_2\zeta(\mathbf{y};\phi). \tag{16}$$

The three normal equations that need to be solved simultaneously to obtain the MPSEs of the unknown parameters are given by

$$\frac{\partial p(\boldsymbol{\vartheta};\mathbf{x},\mathbf{y})}{\partial\gamma_1} = \sum_{i=1}^{J+1}\frac{a_i}{1-e^{-\gamma_1 a_i}}-\eta(\mathbf{x};\phi)=0, \tag{17}$$

$$\frac{\partial p(\boldsymbol{\vartheta};\mathbf{x},\mathbf{y})}{\partial\gamma_2} = \sum_{i=1}^{D+1}\frac{c_i}{1-e^{-\gamma_2 c_i}}-\zeta(\mathbf{y};\phi)=0 \tag{18}$$

and

$$\frac{\partial p(\boldsymbol{\vartheta};\mathbf{x},\mathbf{y})}{\partial\phi} = \gamma_1\sum_{i=1}^{J+1}\frac{a_i^*}{1-e^{-\gamma_1 a_i}}+\gamma_2\sum_{i=1}^{D+1}\frac{c_i^*}{1-e^{-\gamma_2 c_i}}-\gamma_1\eta_1(\mathbf{x};\phi)-\gamma_2\zeta_1(\mathbf{y};\phi)=0, \tag{19}$$

where $a_i^* = x_i^{\phi}\log(x_i) - x_{i-1}^{\phi}\log(x_{i-1})$ and $c_i = y_i^{\phi}\log(y_i) - y_{i-1}^{\phi}\log(y_{i-1})$.

Clearly, in contrast to the likelihood estimation method, closed-form solutions are unavailable for the scale or shape parameters when using the MPS approach. Therefore, to obtain the MPSEs of the unknown parameters, numerical methods such as the Newton-Raphson algorithm must be used. Upon getting the MPSEs, denoted by $\tilde{\gamma}_1, \tilde{\gamma}_1$ and $\tilde{\phi}$, the MPSE of the stress-strength reliability parameter $\mathcal{R}$ can be derived using the invariance property of the MPSEs as follows

$$\widetilde{\mathcal{R}} = \frac{\tilde{\gamma}_1}{\tilde{\gamma}_1 + \tilde{\gamma}_2}.$$

By estimating the variance-covariance matrix based on the MPSEs $\tilde{\boldsymbol{\vartheta}} = (\tilde{\gamma}1, \tilde{\gamma}2, \tilde{\phi})^\top$, and then applying the delta method to approximate the variance of the estimator $\widetilde{\mathcal{R}}$, we can construct the $100\%(1-\alpha)$ ACI for the stress-strength parameter $\mathcal{R}$ in a manner similar to that used in the likelihood estimation approach. Let us first estimate the variance-covariance matrix as follows

$$\boldsymbol{\Sigma}^*(\tilde{\boldsymbol{\vartheta}}) = \begin{bmatrix} -p_{11} & 0 & -p_{13} \\ & -p_{22} & -p_{23} \\ & & -p_{33} \end{bmatrix}^{-1} = \begin{bmatrix} \tilde{V}^*_{11} & 0 & \tilde{V}^*_{13} \\ & \tilde{V}^*_{22} & \tilde{V}^*_{23} \\ & & \tilde{V}^*_{33} \end{bmatrix},$$

where

$$p_{11} = \sum_{i=1}^{J+1} \frac{a_i^2 e^{-\gamma_1 a_i}}{(1 - e^{-\gamma_1 a_i})^2}, \quad p_{22} = \sum_{i=1}^{D+1} \frac{c_i^2 e^{-\gamma_2 c_i}}{(1 - e^{-\gamma_2 c_i})^2},$$

$$p_{33} = \gamma_1 \sum_{i=1}^{J+1} \frac{\nu_i}{1 - e^{-\gamma_1 a_i}} + \gamma_2 \sum_{i=1}^{D+1} \frac{\kappa_i}{1 - e^{-\gamma_2 c_i}} - \gamma_1 \eta_2(\mathbf{x}; \phi) - \gamma_2 \zeta_2(\mathbf{y}; \phi),$$

$$p_{13} = \sum_{i=1}^{J+1} \frac{a_i^*}{1 - e^{-\gamma_1 a_i}} \left(1 - \frac{\gamma_1 a_i e^{-\gamma_1 a_i}}{1 - e^{-\gamma_1 a_i}}\right) - \eta_1(\mathbf{x}; \phi)$$

and

$$p_{23} = \sum_{i=1}^{D+1} \frac{c_i^*}{1 - e^{-\gamma_2 c_i}} \left(1 - \frac{\gamma_2 c_i e^{-\gamma_2 c_i}}{1 - e^{-\gamma_2 c_i}}\right) - \zeta_1(\mathbf{y}; \phi),$$

where $\nu_i = a_i^\star - \dfrac{\gamma_1 a_i^{2*} e^{-\gamma_1 a_i}}{1 - e^{-\gamma_1 a_i}}$, $\kappa_i = c_i^\star - \dfrac{\gamma_2 c_i^{2*} e^{-\gamma_2 c_i}}{1 - e^{-\gamma_2 c_i}}$, $a_i^\star = x_i^\phi \log^2(x_i) - x_{i-1}^\phi \log^2(x_{i-1})$ and $c_i^\star = y_i^\phi \log^2(y_i) - y_{i-1}^\phi \log^2(y_{i-1})$.

Then, by applying the delta method, similar to the approach used in the likelihood estimation discussed in the previous section, the variance of $\mathcal{R}$ can be approximated as follows

$$\tilde{V}_{\mathcal{R}} \approx \frac{\tilde{\gamma}_2^2 \tilde{V}_{11} + \tilde{\gamma}_1^2 \tilde{V}_{22}}{(\tilde{\gamma}_1 + \tilde{\gamma}_2)^2}.$$

The $100\%(1-\alpha)$ ACI of $\mathcal{R}$ in this case can be obtained as

$$\left(\frac{\tilde{\gamma}_1 - z_{\alpha/2}\sqrt{\tilde{\gamma}_2^2 \tilde{V}_{11} + \tilde{\gamma}_1^2 \tilde{V}_{22}}}{\tilde{\gamma}_1 + \tilde{\gamma}_2}, \frac{\tilde{\gamma}_1 + z_{\alpha/2}\sqrt{\tilde{\gamma}_2^2 \tilde{V}_{11} + \tilde{\gamma}_1^2 \tilde{V}_{22}}}{\tilde{\gamma}_1 + \tilde{\gamma}_2}\right).$$

4 Bayesian Estimation

This section focuses on the Bayesian estimation of the stress-strength reliability parameter $\mathcal{R}$ for the Weibull distribution when UTIPHC samples are involved. While classical estimation methods perform well with large or complete samples, they can lead to unreliable results when dealing with small samples or censored data. In such situations, the Bayesian approach offers an advantage by incorporating prior knowledge, often leading to more accurate estimates. The first step in this process is to specify suitable prior distributions for the unknown parameters. From the LF in (6), it is clear that the gamma distribution serves as a conjugate prior for the scale parameters γ_1 and γ_2. However, there is no known conjugate prior for the shape parameter ϕ. Following the approach of Asgharzadeh et al. [5], we also adopt a gamma prior for the shape parameter in this study. Let $\gamma_1 \sim Gamma(b_1, h_1)$, $\gamma_2 \sim Gamma(b_2, h_2)$, and $\phi \sim Gamma(b_3, h_3)$, where the hyper-parameters b_j and h_j, for $j = 1, 2, 3$, are all positive. Then, the joint prior distribution of $\boldsymbol{\vartheta}$ as

$$\pi(\boldsymbol{\vartheta}) \propto \gamma_1^{b_1-1}\gamma_2^{b_2-1}\phi^{b_3-1}\exp\{h_1\gamma_1 - h_2\gamma_2 - h_3\phi\}, \ \gamma_1, \gamma_2, \phi > 0. \tag{20}$$

As mentioned earlier, the Bayes estimators will be obtained using two forms of the posterior distribution. The first is based on the LF, and the second is derived using the SF. By combining the LF in (6) with the prior distribution in (20), we can express the first version of the posterior distribution as follows

$$Q_1(\boldsymbol{\vartheta}|\mathbf{x},\mathbf{y}) = \frac{1}{A_1}\gamma_1^{J+b_1-1}\gamma_2^{D+b_2-1}\phi^{J+D+b_3-1}\exp\{\phi(H - h_3) - \gamma_1[\eta(\mathbf{x};\phi) + h_1] - \gamma_2[\zeta(\mathbf{y};\phi) + h_2]\}, \tag{21}$$

where

$$A_1 = \int_0^\infty\int_0^\infty\int_0^\infty \pi(\boldsymbol{\vartheta})L(\boldsymbol{\vartheta};\mathbf{x},\mathbf{y})d\gamma_1 d\gamma_2 d\phi$$

Likewise, by combining the SF in (15) with prior distribution in (20), the second version of the posterior distribution of the unknown parameters $\boldsymbol{\vartheta}$ can be written as

$$\begin{aligned} Q_2(\boldsymbol{\vartheta}|\mathbf{x},\mathbf{y}) = \frac{1}{A_2}\gamma_1^{b_1-1}\gamma_2^{b_2-1}\phi^{b_3-1}\exp\Bigg\{&\sum_{i=1}^{J+1}\log\left(e^{\gamma_1 a_i} - 1\right) + \sum_{i=1}^{D+1}\log\left(e^{\gamma_2 c_i} - 1\right) \\ &- \gamma_1[\eta(\mathbf{x};\phi) + h_1] - \gamma_2[\zeta(\mathbf{y};\phi) + h_2] - h_3\phi\Bigg\}, \end{aligned} \tag{22}$$

where

$$A_2 = \int_0^\infty\int_0^\infty\int_0^\infty \pi(\boldsymbol{\vartheta})P(\boldsymbol{\vartheta};\mathbf{x},\mathbf{y})d\gamma_1 d\gamma_2 d\phi$$

Let $\widehat{\mathcal{R}}_{LF}$ denote the Bayes estimator of $\mathcal{R} = P(Y < X)$ obtained under the squared error loss function using the posterior distribution in (21). Similarly, let $\widetilde{\mathcal{R}}_{SF}$ represent the Bayes estimator derived from the alternative posterior in (22). Both estimators are calculated as posterior means. However, due to the complex forms of the posterior distributions, these estimators cannot be expressed in closed form. In this study, we utilize numerical approximation methods, particularly the MCMC techniques, to estimate the stress-strength reliability parameter $\mathcal{R}$, including both point estimates and BCIs. To apply the MCMC approach, we begin with the first form of the posterior distribution based on the LF, as given in (21). The initial step is to derive the full conditional distributions, which can be obtained directly from the posterior distribution in (21) as follows

$$Q_1(\gamma_1|\boldsymbol{\vartheta}_{-\gamma_1},\mathbf{x},\mathbf{y}) \propto \gamma_1^{J+b_1-1}\exp\{-\gamma_1[\eta(\mathbf{x};\phi) + h_1]\}, \tag{23}$$

$$Q_1(\gamma_2|\boldsymbol{\vartheta}_{-\gamma_1},\mathbf{x},\mathbf{y}) \propto \gamma_2^{D+b_2-1}\exp\{-\gamma_2[\zeta(\mathbf{y};\phi) + h_2]\}, \tag{24}$$

and

$$Q_1(\phi|\boldsymbol{\vartheta}_{-\phi}, \mathbf{x}, \mathbf{y}) \propto \phi^{J+D+b_3-1} \exp\{\phi(H-h_3) - \gamma_1[\eta(\mathbf{x};\phi)+h_1] - \gamma_2[\zeta(\mathbf{y};\phi)+h_2]\}. \tag{25}$$

It is evident from (23) and (24) that the conditional distributions of γ_1 and γ_2 are gamma-distributed, allowing for straightforward sampling. However, the full conditional distribution of ϕ, given by (25), does not belong to any standard distributional family. As a result, we adopt the Metropolis-Hastings (M-H) algorithm with a normal proposal distribution within the Gibbs sampling framework to generate the required MCMC samples. The sampling procedure can be implemented by following the steps outlined in Algorithm 1.

Algorithm 1: The MCMC Sampling Procedure

Step 1. Put $j = 1$ and $\left(\gamma_1^{(0)}, \gamma_2^{(0)}, \phi^{(0)}\right) = (\hat{\gamma}_1, \hat{\gamma}_2, \hat{\phi})$.
Step 2. Simulate a candidate value $\phi^{(j)}$ using $Q_1(\phi|\boldsymbol{\vartheta}_{-\phi}, \mathbf{x}, \mathbf{y})$ using the M-H seps:
- Get ϕ^* using $N\left(\phi^{(j-1)}, \hat{V}_{33}\right)$.
- Calculate the acceptance ratio:

$$\psi = \min\left[1, \frac{Q_1(\phi^*|\boldsymbol{\vartheta}_{-\phi}^{(j-1)}, \underline{\mathbf{x}}, \underline{\mathbf{y}})}{Q_1(\phi^{(j-1)}|\boldsymbol{\vartheta}_{-\phi}^{(j-1)}, \underline{\mathbf{x}}, \underline{\mathbf{y}})}\right].$$

- Obtain u, $u \sim U(0, 1)$.
- Put $\phi^{(j)} = \phi^*$ if $u \leq \psi$, or $\phi^{(j)} = \phi^{(j-1)}$, otherwise.

Step 3. Use the updated value of $\phi^{(j)}$ to generate:
- $\gamma_1^{(j)}$ from *Gamma* $\left(J + b_1, \eta(\mathbf{x}; \phi^{(j)}) + h_1\right)$.
- $\gamma_2^{(j)}$ from *Gamma* $\left(D + b_2, \zeta(\mathbf{y}; \phi^{(j)}) + h_2\right)$.

Step 4. At iteration j, calculate $\mathcal{R}$ as:

$$\mathcal{R}^{(j)} = \frac{\gamma_1^{(j)}}{\gamma_1^{(j)} + \gamma_2^{(j)}}.$$

Step 5. Set $j = j + 1$.
Step 6. Redo Steps 2 to 5, $\mathcal{M}$ times to compute $\left\{\mathcal{R}^{(1)}, \mathcal{R}^{(2)}, \ldots, \mathcal{R}^{(\mathcal{M})}\right\}$.

Using the MCMC samples generated, and applying the squared error loss function, the Bayes estimate of the stress-strength reliability parameter $\mathcal{R}$ can be obtained. After discarding the initial $\mathcal{B}$ samples as a burn-in period, the Bayes estimate can be computed using the remaining MCMC samples, denoted by $\bar{\mathcal{M}}$, as

$$\hat{\mathcal{R}}_{LF} = \frac{1}{\bar{\mathcal{M}}} \sum_{j=1}^{\bar{\mathcal{M}}} \mathcal{R}^{(j)}, \quad \bar{\mathcal{M}} = \mathcal{M} - \mathcal{B}.$$

After sorting the remaining samples of size $\bar{\mathcal{M}}$ as $\left\{\mathcal{R}^{[1]}, \mathcal{R}^{[2]}, \ldots, \mathcal{R}^{[\bar{\mathcal{M}}]}\right\}$, we can construct the $100\%(1-\alpha)$ BCI of $\mathcal{R}$ as

$$\left\{\mathcal{R}^{[\alpha\bar{\mathcal{M}}/2]}, \mathcal{R}^{[(1-\alpha/2)\bar{\mathcal{M}}]}\right\}.$$

To obtain the Bayes estimate of $\mathcal{R}$ using the second version of the posterior distribution derived using the SF, we first need to derive the full conditional distributions of γ_1, γ_2 and ϕ based on the posterior distribution in (22) as follows

$$Q_2(\gamma_1|\boldsymbol{\vartheta}_{-\gamma_1},\mathbf{x},\mathbf{y}) \propto \gamma_1^{b_1-1}\exp\left\{\sum_{i=1}^{J+1}\log\left(e^{\gamma_1 a_i}-1\right)-\gamma_1[\eta(\mathbf{x};\phi)+h_1]\right\}, \tag{26}$$

$$Q_2(\gamma_2|\boldsymbol{\vartheta}_{-\gamma_2},\mathbf{x},\mathbf{y}) \propto \gamma_2^{b_2-1}\exp\left\{\sum_{i=1}^{D+1}\log\left(e^{\gamma_2 c_i}-1\right)-\gamma_2[\zeta(\mathbf{y};\phi)\right\} \tag{27}$$

and

$$Q_2(\phi|\boldsymbol{\vartheta}_{-\phi},\mathbf{x},\mathbf{y}) \propto \phi^{b_3-1}\exp\left\{\sum_{i=1}^{J+1}\log\left(e^{\gamma_1 a_i}-1\right)+\sum_{i=1}^{D+1}\log\left(e^{\gamma_2 c_i}-1\right)\right.$$
$$\left.-\gamma_1\eta(\mathbf{x};\phi)-\gamma_2\zeta(\mathbf{y};\phi)-h_3\phi\right\}. \tag{28}$$

It is obvious that the three conditional distributions presented by (26)–(28) do not correspond to any common probability distributions. Consequently, we operate the M-H algorithm utilizing a normal proposal distribution for each parameter, as represented in Step 2 of Algorithm 1, to yield the required MCMC samples. Algorithm 2 summarizes the steps of M-H sampling process.

Algorithm 2: The M-H Sampling for Stress-Stress Reliability

Step 1. Set $j=1$ and $\left(\gamma_1^{(0)},\gamma_2^{(0)},\phi^{(0)}\right)=(\tilde{\gamma}_1,\tilde{\gamma}_2,\tilde{\phi})$.
Step 2. Use the M-H algorithm as discussed in Step 2 in Algorithm 1 to obtain:
- $\gamma_1^{(j)}$ from $Q_2(\gamma_1|\boldsymbol{\vartheta}_{-\gamma_1},\mathbf{x},\mathbf{y})$ using $N\left(\gamma_1^{(j-1)},\hat{V}_{11}\right)$.
- $\gamma_2^{(j)}$ from $Q_2(\gamma_2|\boldsymbol{\vartheta}_{-\gamma_2},\mathbf{x},\mathbf{y})$ with $N\left(\gamma_2^{(j-1)},\hat{V}_{22}\right)$.
- $\phi^{(j)}$ from $Q_2(\phi|\boldsymbol{\vartheta}_{-\phi},\mathbf{x},\mathbf{y})$ with $N\left(\phi^{(j-1)},\hat{V}_{33}\right)$.

Step 3. Compute $\mathcal{R}$ at iteration number j as:
$$\mathcal{R}^{*(j)}=\frac{\gamma_1^{(j)}}{\gamma_1^{(j)}+\gamma_2^{(j)}}.$$
Step 4. Update j by $j+1$.
Step 5. Redo Steps 2 to 4 $\mathcal{M}$ times to compute $\left\{\mathcal{R}^{*(1)},\mathcal{R}^{*(2)},\ldots,\mathcal{R}^{*(\mathcal{M})}\right\}$.

Similar to the case of obtaining the Bayes estimate using the LF, we can obtain the Bayes estimate of $\mathcal{R}$ using the posterior distribution derived based on the SF, after the burn-in period $\mathcal{B}$, as follows

$$\hat{\mathcal{R}}_{SF}=\frac{1}{\bar{\mathcal{M}}}\sum_{j=1}^{\bar{\mathcal{M}}}\mathcal{R}^{*(j)}.$$

In addition, by sorting the remaining MCMC samples as $\left\{\mathcal{R}^{*[1]},\mathcal{R}^{*[2]},\ldots,\mathcal{R}^{[*\bar{\mathcal{M}}]}\right\}$, the $100\%(1-\alpha)$ BCI of $\mathcal{R}$ follows

$$\left\{\mathcal{R}^{*[\alpha\bar{\mathcal{M}}/2]},\mathcal{R}^{*[(1-\alpha/2)\bar{\mathcal{M}}]}\right\}.$$

5 Numerical Comparisons

This section presents an extensive Monte Carlo simulation study designed to validate the estimators derived from the established theoretical results discussed earlier. To rigorously examine the behavior of both point and interval estimators for the parameters γ_i, $i = 1, 2, \phi$, and the stress-strength reliability index $\mathcal{R}$, we implemented a simulation experiment utilizing 1000 independent UTIPHC samples generated from $\mathrm{W}(\gamma_1, \gamma_2, \phi) = (0.5, 1.5, 0.5)$ distribution. Subsequently, the true value of $\mathcal{R}$ corresponding to the specified population is assumed to be $\frac{1}{4}$. To make a comprehensive comparison, we incorporate several simulation setups characterized by censoring vectors **R** and **Q**, along with varying settings for total sample sizes (n_i, n_i^*), number of effective observations (m_i, m_i^*), and censoring termination bounds (T_i and T_i^*) for $i = 1, 2$. These experimental settings are comprehensively summarized in Table 2. For each configuration listed in Table 2, two distinct termination time intervals (T_i and T_i^*) for $i = 1, 2$ are considered, such as $T_1 = T_1^*$ (=0.5, 1.5) and $T_2 = T_2^*$ (=1, 2). The study evaluates four different progressive Type-II censoring patterns. These strategies reflect various censoring layouts, including left, middle, and right censoring schemes. For instance, from Group X, a censoring pattern such as $\{(2^{\star}5, 0^{\star}5)\}$ indicates that two survivors are randomly selected and withdrawn from the test, and then no survivors are removed until the test is stopped.

Table 2: Comparison frameworks in Monte Carlo simulation

Test	Group X			Group Y		
	n	(k, m)	**R**	n^*	(k^*, m^*)	**S**
A1	20	(5, 10)	$(2^{\star}5, 0^{\star}5)$	30	(10, 15)	$(3^{\star}5, 0^{\star}10)$
A2			$(0^{\star}2, 2^{\star}5, 0^{\star}3)$			$(0^{\star}5, 3^{\star}5, 0^{\star}5)$
A3			$(0^{\star}5, 2^{\star}5)$			$(0^{\star}10, 3^{\star}5)$
A4		(10, 15)	$(1^{\star}5, 0^{\star}10)$		(15, 20)	$(2^{\star}5, 0^{\star}15)$
A5			$(0^{\star}5, 1^{\star}5, 0^{\star}5)$			$(0^{\star}7, 2^{\star}5, 0^{\star}8)$
A6			$(0^{\star}10, 1^{\star}5)$			$(0^{\star}15, 2^{\star}5)$
B1	40	(10, 20)	$(2^{\star}10, 0^{\star}10)$	50	(20, 30)	$(2^{\star}10, 0^{\star}20)$
B2			$(0^{\star}5, 2^{\star}10, 0^{\star}5)$			$(0^{\star}10, 2^{\star}10, 0^{\star}10)$
B3			$(0^{\star}10, 2^{\star}10)$			$(0^{\star}20, 2^{\star}10)$
B4		(20, 30)	$(1^{\star}10, 0^{\star}20)$		(30, 40)	$(1^{\star}10, 0^{\star}30)$
B5			$(0^{\star}10, 1^{\star}10, 0^{\star}10)$			$(0^{\star}15, 1^{\star}10, 0^{\star}15)$
B6			$(0^{\star}20, 1^{\star}10)$			$(0^{\star}30, 1^{\star}10)$
C1	60	(20, 40)	$(2^{\star}10, 0^{\star}30)$	70	(30, 50)	$(2^{\star}10, 0^{\star}40)$
C2			$(0^{\star}15, 2^{\star}10, 0^{\star}15)$			$(0^{\star}20, 2^{\star}10, 0^{\star}20)$
C3			$(0^{\star}30, 2^{\star}10)$			$(0^{\star}40, 2^{\star}10)$
C4		(30, 50)	$(1^{\star}10, 0^{\star}40)$		(40, 60)	$(1^{\star}10, 0^{\star}50)$
C5			$(0^{\star}20, 1^{\star}10, 0^{\star}20)$			$(0^{\star}25, 1^{\star}10, 0^{\star}25)$
C6			$(0^{\star}40, 1^{\star}10)$			$(0^{\star}50, 1^{\star}10)$

After assigning the values of n_i, n_i^*, m_i, m_i^*, k_i, k_i^*, T_1, T_1^*, T_2, T_2^* (for $i = 1, 2$), **R**, and **S**, to generate a UTIPHC sample, do the next procedure:

Step 1: Set the true values of $\mathrm{W}(\gamma_1, \phi)$ population model.

Step 2: Simulate a progressive Type-II censored dataset as:

(a) Simulate q independent random variables $q_1, q_2, \ldots, q_m$ from uniform $U(0, 1)$ distribution.

(b) Compute $\varrho_i = q_i^{\left(i+\sum_{j=m-i+1}^{m} R_j\right)^{-1}}$ for $i = 1, 2, \ldots, m$.

(c) Obtain $U_i = 1 - \prod_{j=m-i+1}^{m} \varrho_j$ for $i = 1, 2, \ldots, m$.

(d) Generate a progressive Type-II censored sample of size m from the $\mathrm{W}(\gamma_1, \phi)$ distribution using the inversion method:

$$X_i = \left[-\frac{1}{\gamma_1}\log\left(1 - \log(u_i)\right)\right]^{\frac{1}{\phi}}, \quad i = 1, 2, \ldots, m.$$

Step 3: Identify d_i at T_i (for $i = 1, 2$).

Step 4: Identify the UTIPHC data type as:

a. Case-1: If $X_{k:n} < X_{m:n} < T_1 < T_2$; stop the test at $X_{m:n}$;
b. Case-2: If $X_{k:n} < T_1 < X_{m:n} < T_2$ (or $X_{k:n} < T_1 < T_2 < X_{m:n}$); stop the test at T_1;
c. Case-3: If $T_1 < X_{k:n} < X_{m:n} < T_2$ (or $T_1 < X_{k:n} < T_2 < X_{m:n}$); stop the test at $X_{k:n}$;
d. Case-4: If $T_1 < T_2 < X_{k:n} < X_{m:n}$; stop the test at T_2.

Step 5: Redo Steps 1–4 for the $\mathrm{W}(\gamma_2, \phi)$ population.

To specify the hyperparameters b_i and h_i $(i = 1, 2)$ governing the joint gamma prior distribution on the scale parameters γ_i, $i = 1, 2$, based on the approach of synthetically generated historical datasets suggested by Nassar and Elshahhat [29]. By gathering 10,000 past complete datasets, each with size 50, when $(b_3, h_3) = (1, 2)$ is taken as without loss of generality, the hyperparameter values (b_1, b_2, h_1, h_2) of γ_i, $i = 1, 2$, are assigned to be:

- (75.7121, 77.8578, 147.383, 50.4344) from LF;
- (73.0298, 75.6217, 134.167, 46.3773) from SF.

To implement the MCMC procedure outlined in Section 4, we generate a total of 12,000 iterations for each simulation run. The initial 2000 samples are discarded as burn-in to reduce the sensitivity to initial starting values and ensure convergence of the chain. The remaining 10,000 post-burn-in samples, derived under both the LF-based and SF-based Bayesian frameworks, are utilized to compute the posterior samples. From these retained samples, Bayes MCMC and corresponding 95% BCI estimates are obtained for the model parameters ϕ and γ_i, $i = 1, 2$, and the stress-strength reliability measure $\mathcal{R}$.

Once the generation of 1000 UTIPHC samples is collected, we conduct the estimation of the parameters γ_i, $i = 1, 2$, ϕ, and the stress-strength reliability measure $\mathcal{R}$ using two well-established packages within the programming environment (version 4.2.2) by R Core Team [30]:

- The package, introduced by Henningsen and Toomet [31], is employed to derive the ML and MPS estimates. This package is also utilized to estimate the two bounds of ACI-LF and ACI-SF.

- The package, developed by Plummer et al. [32], supports the Bayesian analysis by offering a comprehensive suite of functions for assessing convergence diagnostics and extracting posterior summaries from MCMC output for all targeted parameters.

Specifically, the average point estimate (APE) of ϕ (for example) is computed as

$$\mathrm{APE}(\ddot{\phi}) = \frac{1}{1000}\sum_{i=1}^{1000}\ddot{\phi}^{[i]},$$

where $\ddot{\phi}^{[i]}$ denotes the computed point estimate of ϕ at ith simulated sample.

Next, two metrics of point assessments, namely root mean squared error (RMSE) and average relative absolute bias (ARAB), are performed to see the superiority of ϕ, respectively, as

$$\mathrm{RMSE}(\ddot{\phi}) = \sqrt{\frac{1}{1000}\sum\nolimits_{i=1}^{1000}\left(\ddot{\phi}^{[i]}-\phi\right)^2},$$

and

$$\mathrm{ARAB}(\ddot{\phi}) = \frac{1}{1000}\sum\nolimits_{i=1}^{1000}\phi^{-1}\left|\ddot{\phi}^{[i]}-\phi\right|,$$

Additionally, two metrics of interval assessments at a significance percentage 5%, namely average interval length (AIL) and coverage percentage (CP) are also considered as

$$\mathrm{AIL}_{95\%}(\phi) = \frac{1}{1000}\sum\nolimits_{i=1}^{1000}\left(\mathcal{U}_{\ddot{\phi}^{[i]}}-\mathcal{L}_{\ddot{\phi}^{[i]}}\right)$$

and

$$\mathrm{CP}_{95\%}(\phi) = \frac{1}{1000}\sum\nolimits_{i=1}^{1000}\mathbb{D}^{\bullet}_{\left(\mathrm{L}_{\ddot{\phi}^{[i]}};\mathrm{U}_{\ddot{\phi}^{[i]}}\right)}(\phi),$$

respectively, where $\mathbb{D}^{\bullet}(\cdot)$ is the indicator function and $(\mathrm{L}(\cdot),\mathrm{U}(\cdot))$ denotes the (lower, upper) sides of the 95% ACI (or BCI) estimate of ϕ.

Tables 3–10 present the key performance metrics used to evaluate the proposed estimation approaches. Specifically, Tables 3–6 report the RMSEs and ARABs in the first and second columns, respectively, while Tables 7–10 list the AILs and CPs in the first and second columns, respectively. As a result, based on estimation accuracy (minimized RMSE, ARAB, and AIL) and reliability (maximized CP), we report the following assessments:

- Overall, the proposed estimators for γ_i $(i = 1, 2)$, ϕ, and the stress-strength reliability measure $\mathcal{R}$ demonstrate efficient and precise performance under various configurations.
- Estimation accuracy improves notably when n (or m) increases, as well as when the total number of censored observations $\sum_{i=1}^{m} R_i$ (or $\sum_{i=1}^{m^*} S_i$) decreases. The same behavior is also reached when n^* (or m^*) increases.
- Extending the predefined experimental thresholds T_1, T_1^*, T_2, T_2^* (for $i = 1, 2$) helped us to enhance estimator precision. Consequently, for practitioners constrained by testing resources, maximizing test durations is advisable to achieve more reliable inference.
- The Bayesian MCMC estimators against LF-based (or SF-based), incorporating informative gamma priors, consistently outperform frequentist in both point and interval scenarios.
- A comparative analysis of estimation techniques yields the following insights:

- For point estimation approaches:
  - For γ_i $(i = 1, 2)$ and ϕ, the MPS approach outperforms the ML approach, whereas ML proves superior to its competitor ML approach, for estimating $\mathcal{R}$;
  - For γ_i $(i = 1, 2)$ and ϕ, the Bayes method using an SF-based approach outperforms its competitor using an LF-based approach, whereas the Bayes method using an SF-based approach is superior to its competitor using an LF-based approach for estimating $\mathcal{R}$.
- For interval estimation approaches:
  - The ACI from SF-based offers superior performance for γ_i and ϕ, whereas the ACI using LF-based is more effective for $\mathcal{R}$;
  - The BCI from SF-based offers superior performance for γ_i and ϕ, whereas the BCI using LF-based is more effective for $\mathcal{R}$.

- Assessing the proposed progressive censoring plans (listed in Table 2):
  - Estimates of γ_i, $i = 1, 2$ show improved performance based on right–censoring used in Ai, Bi, and Ci for $i = 3, 6$;
  - Estimates of ϕ show improved performance based on middle censoring used in Ai, Bi, and Ci for $i = 2, 5$;
  - Estimates of $\mathcal{R}$ show improved performance based on left-censoring used in Ai, Bi, and Ci for $i = 1, 4$.
- In summary, when a researcher or reliability practitioner is interested in analyzing data structured by the UTIPHC sampling framework, the Bayes MCMC approach using LF-based is recommended for estimating the Weibull stress-strength parameter. In contrast, the Bayes MCMC approach using SF-based is recommended for estimating the Weibull model parameters.

Table 3: Point assessments of γ_1

Test	MLE			MPSE			MCMC (LF-based)			MCMC (SF-based)		
					$\{(T_1, T_2, T_1^*, T_2^*)\} = \{(0.5, 1.0, 0.5, 1.0)\}$							
A1	0.596	0.435	0.791	0.455	0.394	0.657	0.524	0.350	0.622	0.559	0.325	0.461
A2	0.620	0.524	1.244	0.466	0.508	0.860	0.524	0.371	0.714	0.560	0.333	0.638
A3	0.567	0.472	0.965	0.422	0.437	0.796	0.528	0.369	0.691	0.563	0.329	0.629
A4	0.601	0.339	0.628	0.487	0.307	0.564	0.540	0.217	0.349	0.549	0.157	0.246
A5	0.670	0.343	0.637	0.137	0.313	0.573	0.531	0.279	0.532	0.540	0.193	0.295
A6	0.705	0.342	0.635	0.562	0.311	0.570	0.555	0.259	0.377	0.566	0.187	0.284
B1	0.537	0.307	0.579	0.462	0.294	0.523	0.547	0.141	0.223	0.609	0.124	0.188
B2	0.564	0.318	0.585	0.478	0.297	0.538	0.552	0.161	0.304	0.612	0.129	0.199
B3	0.543	0.312	0.582	0.462	0.296	0.535	0.552	0.147	0.254	0.614	0.127	0.198
B4	0.548	0.298	0.548	0.487	0.289	0.516	0.581	0.117	0.182	0.642	0.100	0.163
B5	0.545	0.300	0.564	0.484	0.292	0.521	0.580	0.128	0.186	0.640	0.109	0.171
B6	0.544	0.305	0.565	0.487	0.293	0.522	0.577	0.132	0.213	0.624	0.111	0.172
C1	0.521	0.279	0.528	0.471	0.270	0.487	0.561	0.101	0.157	0.559	0.086	0.139

(Continued)

Table 3 (continued)

C2	0.525	0.282	0.535	0.472	0.279	0.499	0.564	0.109	0.167	0.563	0.087	0.141
C3	0.532	0.293	0.535	0.480	0.282	0.515	0.553	0.114	0.178	0.554	0.096	0.150
C4	0.586	0.266	0.490	0.490	0.255	0.463	0.610	0.080	0.128	0.588	0.068	0.110
C5	0.513	0.273	0.509	0.488	0.260	0.473	0.610	0.083	0.133	0.586	0.072	0.115
C6	0.534	0.277	0.518	0.492	0.266	0.486	0.606	0.085	0.136	0.584	0.073	0.118
$\{(T_1, T_2, T_1^*, T_2^*)\} = \{(1.5, 2.0, 1.5, 2.0)\}$												
A1	0.596	0.430	0.781	0.447	0.350	0.657	0.519	0.326	0.621	0.554	0.248	0.299
A2	0.566	0.517	0.980	0.439	0.505	0.845	0.528	0.368	0.690	0.564	0.330	0.630
A3	0.576	0.457	0.835	0.482	0.431	0.782	0.542	0.352	0.660	0.576	0.329	0.622
A4	0.562	0.322	0.594	0.464	0.302	0.539	0.547	0.174	0.250	0.550	0.142	0.230
A5	0.484	0.339	0.629	0.575	0.312	0.572	0.562	0.206	0.298	0.577	0.168	0.276
A6	0.635	0.329	0.612	0.135	0.307	0.564	0.535	0.193	0.286	0.536	0.159	0.261
B1	0.527	0.305	0.578	0.454	0.292	0.523	0.552	0.126	0.204	0.609	0.115	0.186
B2	0.530	0.309	0.583	0.459	0.296	0.537	0.544	0.132	0.221	0.600	0.129	0.210
B3	0.528	0.307	0.582	0.462	0.294	0.531	0.536	0.128	0.208	0.585	0.126	0.196
B4	0.529	0.297	0.538	0.473	0.279	0.501	0.564	0.114	0.164	0.625	0.098	0.157
B5	0.538	0.300	0.541	0.479	0.285	0.503	0.581	0.117	0.171	0.640	0.105	0.170
B6	0.540	0.302	0.541	0.484	0.287	0.511	0.577	0.123	0.174	0.624	0.111	0.170
C1	0.577	0.272	0.509	0.470	0.270	0.482	0.539	0.094	0.154	0.538	0.082	0.132
C2	0.546	0.282	0.528	0.470	0.274	0.493	0.546	0.099	0.158	0.549	0.085	0.140
C3	0.526	0.289	0.530	0.469	0.279	0.505	0.564	0.099	0.159	0.560	0.092	0.147
C4	0.548	0.256	0.482	0.478	0.253	0.456	0.614	0.076	0.120	0.592	0.067	0.108
C5	0.521	0.260	0.486	0.480	0.258	0.464	0.606	0.077	0.126	0.587	0.071	0.115
C6	0.526	0.267	0.507	0.486	0.264	0.469	0.606	0.079	0.128	0.584	0.072	0.116

Table 4: Point assessments of γ_2

Test	MLE			MPSE			MCMC (LF-based)			MCMC (SF-based)		
$\{(T_1, T_2, T_1^*, T_2^*)\} = \{(0.5, 1.0, 0.5, 1.0)\}$												
A1	1.756	0.751	0.399	1.442	0.535	0.324	1.688	0.242	0.181	1.554	0.162	0.093
A2	1.965	0.840	0.529	1.602	0.663	0.484	1.692	0.247	0.214	1.556	0.172	0.101
A3	1.858	0.774	0.429	1.563	0.687	0.350	1.687	0.249	0.194	1.549	0.176	0.098
A4	1.401	0.658	0.340	1.213	0.389	0.205	1.486	0.228	0.153	1.520	0.125	0.063
A5	1.336	0.729	0.382	1.302	0.423	0.252	1.443	0.234	0.178	1.485	0.139	0.069
A6	1.848	0.684	0.360	1.570	0.416	0.234	1.537	0.231	0.163	1.583	0.133	0.067
B1	1.735	0.555	0.297	1.533	0.324	0.174	1.678	0.218	0.129	1.571	0.114	0.058
B2	1.981	0.657	0.339	1.744	0.365	0.186	1.686	0.228	0.142	1.582	0.120	0.062
B3	1.746	0.579	0.330	1.535	0.336	0.179	1.676	0.221	0.135	1.575	0.115	0.059

(Continued)

Table 4 **(continued)**

B4	1.383	0.492	0.268	1.277	0.255	0.140	1.668	0.177	0.111	1.576	0.104	0.054
B5	1.048	0.538	0.275	1.406	0.269	0.145	1.587	0.198	0.118	1.497	0.110	0.058
B6	1.285	0.496	0.272	1.395	0.263	0.141	1.658	0.183	0.115	1.559	0.108	0.057
C1	1.658	0.438	0.233	1.515	0.215	0.118	1.727	0.140	0.058	1.651	0.083	0.047
C2	1.532	0.472	0.245	1.415	0.246	0.135	1.720	0.167	0.108	1.639	0.102	0.052
C3	1.660	0.467	0.240	1.514	0.234	0.133	1.725	0.157	0.092	1.647	0.087	0.052
C4	1.280	0.328	0.162	1.205	0.176	0.091	1.660	0.106	0.018	1.570	0.042	0.019
C5	1.276	0.414	0.228	1.317	0.213	0.117	1.599	0.128	0.043	1.496	0.074	0.038
C6	1.242	0.364	0.178	1.173	0.183	0.099	1.653	0.117	0.034	1.560	0.049	0.025
						$\{(T_1, T_2, T_1^*, T_2^*)\} = \{(1.5, 2.0, 1.5, 2.0)\}$						
A1	1.646	0.656	0.393	1.410	0.495	0.293	1.688	0.279	0.147	1.549	0.139	0.074
A2	1.564	0.684	0.964	1.359	0.647	0.791	1.690	0.343	0.155	1.551	0.164	0.078
A3	1.638	0.714	0.763	1.478	0.680	0.345	1.681	0.293	0.150	1.543	0.144	0.077
A4	1.564	0.490	0.270	1.390	0.375	0.204	1.534	0.230	0.136	1.580	0.118	0.061
A5	1.305	0.586	0.363	1.208	0.412	0.225	1.538	0.252	0.140	1.568	0.135	0.068
A6	1.406	0.571	0.357	1.309	0.404	0.211	1.478	0.241	0.138	1.526	0.121	0.066
B1	1.531	0.479	0.249	1.410	0.319	0.166	1.680	0.218	0.128	1.571	0.112	0.058
B2	1.542	0.484	0.270	1.408	0.342	0.182	1.678	0.226	0.134	1.568	0.117	0.060
B3	1.555	0.481	0.257	1.427	0.333	0.175	1.685	0.219	0.129	1.575	0.114	0.059
B4	1.436	0.452	0.244	1.347	0.245	0.126	1.672	0.173	0.105	1.579	0.092	0.047
B5	1.737	0.472	0.247	1.402	0.261	0.135	1.587	0.182	0.112	1.497	0.110	0.057
B6	1.290	0.456	0.245	1.211	0.258	0.132	1.666	0.174	0.106	1.570	0.097	0.051
C1	1.544	0.431	0.204	1.460	0.196	0.105	1.700	0.094	0.058	1.617	0.071	0.036
C2	1.463	0.449	0.242	1.385	0.242	0.126	1.697	0.162	0.102	1.611	0.084	0.040
C3	1.533	0.438	0.235	1.441	0.224	0.117	1.698	0.118	0.066	1.616	0.080	0.040
C4	1.419	0.257	0.133	1.355	0.167	0.089	1.662	0.058	0.015	1.577	0.029	0.009
C5	1.579	0.358	0.178	1.413	0.184	0.096	1.638	0.078	0.039	1.534	0.067	0.030
C6	1.359	0.291	0.153	1.294	0.183	0.094	1.677	0.072	0.032	1.594	0.031	0.018

Table 5: Point assessments of ϕ

Test	MLE			MPSE			MCMC (LF-based)			MCMC (SF-based)		
						$\{(T_1, T_2, T_1^*, T_2^*)\} = \{(0.5, 1.0, 0.5, 1.0)\}$						
A1	0.614	0.916	0.898	0.550	0.484	0.285	0.422	0.218	0.271	0.458	0.216	0.253
A2	0.546	0.430	0.609	0.508	0.427	0.238	0.435	0.200	0.217	0.466	0.180	0.179
A3	0.640	0.894	0.771	0.459	0.451	0.254	0.461	0.208	0.247	0.489	0.182	0.219
A4	0.613	0.213	0.332	0.613	0.192	0.204	0.432	0.167	0.190	0.478	0.133	0.164
A5	0.483	0.189	0.254	0.480	0.167	0.180	0.449	0.160	0.167	0.498	0.106	0.144

(Continued)

Table 5 **(continued)**

A6	0.696	0.194	0.278	0.724	0.183	0.189	0.581	0.164	0.186	0.563	0.129	0.157
B1	0.609	0.169	0.242	0.575	0.158	0.174	0.472	0.149	0.149	0.580	0.090	0.129
B2	0.535	0.155	0.206	0.516	0.145	0.163	0.455	0.124	0.139	0.558	0.086	0.122
B3	0.548	0.157	0.222	0.520	0.150	0.165	0.465	0.129	0.141	0.569	0.089	0.127
B4	0.477	0.138	0.170	0.483	0.106	0.152	0.426	0.096	0.133	0.443	0.078	0.116
B5	0.505	0.099	0.161	0.506	0.082	0.137	0.508	0.079	0.125	0.543	0.070	0.112
B6	0.496	0.106	0.165	0.499	0.087	0.149	0.491	0.082	0.130	0.513	0.071	0.114
C1	0.527	0.097	0.157	0.519	0.079	0.129	0.466	0.075	0.121	0.539	0.065	0.103
C2	0.530	0.086	0.136	0.519	0.069	0.113	0.490	0.057	0.091	0.564	0.034	0.057
C3	0.533	0.089	0.144	0.520	0.070	0.118	0.491	0.068	0.106	0.564	0.046	0.075
C4	0.471	0.083	0.129	0.476	0.066	0.109	0.365	0.048	0.084	0.390	0.034	0.056
C5	0.496	0.078	0.116	0.497	0.062	0.098	0.429	0.029	0.048	0.459	0.027	0.041
C6	0.493	0.080	0.122	0.495	0.065	0.103	0.424	0.045	0.079	0.452	0.027	0.045
$\{(T_1, T_2, T_1^*, T_2^*)\} = \{(1.5, 2.0, 1.5, 2.0)\}$												
A1	0.515	0.522	0.823	0.497	0.478	0.279	0.422	0.212	0.263	0.454	0.206	0.252
A2	0.520	0.428	0.466	0.527	0.311	0.222	0.419	0.197	0.198	0.452	0.175	0.172
A3	0.425	0.466	0.728	0.479	0.429	0.247	0.473	0.200	0.242	0.499	0.179	0.183
A4	0.479	0.198	0.225	0.519	0.179	0.202	0.590	0.147	0.180	0.631	0.115	0.164
A5	0.501	0.184	0.217	0.509	0.162	0.174	0.537	0.131	0.151	0.579	0.096	0.129
A6	0.432	0.191	0.220	0.134	0.165	0.188	0.475	0.139	0.159	0.518	0.106	0.134
B1	0.511	0.165	0.203	0.504	0.155	0.169	0.453	0.129	0.138	0.552	0.084	0.119
B2	0.511	0.148	0.181	0.504	0.138	0.148	0.461	0.114	0.129	0.562	0.080	0.110
B3	0.510	0.154	0.189	0.509	0.149	0.162	0.449	0.116	0.131	0.551	0.083	0.115
B4	0.484	0.115	0.156	0.490	0.097	0.146	0.426	0.085	0.124	0.443	0.074	0.100
B5	0.502	0.090	0.148	0.510	0.079	0.127	0.494	0.075	0.118	0.522	0.037	0.063
B6	0.496	0.092	0.151	0.500	0.082	0.141	0.500	0.076	0.121	0.525	0.065	0.094
C1	0.507	0.085	0.143	0.508	0.075	0.122	0.437	0.073	0.116	0.511	0.036	0.060
C2	0.509	0.079	0.121	0.514	0.066	0.108	0.419	0.051	0.082	0.484	0.030	0.053
C3	0.511	0.081	0.127	0.511	0.070	0.113	0.427	0.055	0.097	0.499	0.034	0.057
C4	0.498	0.076	0.117	0.503	0.065	0.105	0.406	0.046	0.081	0.433	0.026	0.041
C5	0.510	0.070	0.107	0.517	0.060	0.095	0.447	0.027	0.043	0.473	0.022	0.032
C6	0.508	0.072	0.111	0.512	0.063	0.100	0.460	0.028	0.045	0.485	0.023	0.036

Table 6: Point assessments of $\mathcal{R}$

Test	MLE			MPSE			MCMC (LF-based)			MCMC (SF-based)		
$\{(T_1, T_2, T_1^*, T_2^*)\} = \{(0.5, 1.0, 0.5, 1.0)\}$												
A1	0.259	0.134	0.445	0.245	0.220	0.820	0.300	0.088	0.326	0.327	0.110	0.390

(Continued)

Table 6 (continued)

A2	0.245	0.277	1.012	0.230	0.524	1.214	0.299	0.095	0.342	0.327	0.119	0.418
A3	0.478	0.222	0.819	0.454	0.339	1.028	0.301	0.091	0.341	0.329	0.113	0.398
A4	0.327	0.090	0.314	0.309	0.106	0.358	0.331	0.076	0.229	0.330	0.081	0.296
A5	0.096	0.105	0.371	0.290	0.116	0.418	0.335	0.086	0.316	0.333	0.094	0.361
A6	0.281	0.102	0.360	0.268	0.113	0.405	0.329	0.082	0.260	0.326	0.087	0.314
B1	0.243	0.087	0.274	0.238	0.089	0.337	0.307	0.067	0.214	0.339	0.076	0.260
B2	0.241	0.088	0.288	0.235	0.091	0.341	0.308	0.068	0.217	0.340	0.077	0.275
B3	0.227	0.089	0.313	0.220	0.102	0.355	0.307	0.071	0.227	0.339	0.081	0.292
B4	0.297	0.081	0.269	0.288	0.084	0.315	0.318	0.052	0.168	0.348	0.063	0.228
B5	0.350	0.085	0.272	0.337	0.088	0.332	0.328	0.055	0.174	0.355	0.067	0.240
B6	0.305	0.082	0.270	0.295	0.086	0.322	0.319	0.053	0.173	0.350	0.064	0.231
C1	0.243	0.068	0.217	0.240	0.079	0.290	0.306	0.042	0.127	0.315	0.059	0.204
C2	0.242	0.071	0.222	0.240	0.082	0.308	0.307	0.047	0.154	0.317	0.060	0.206
C3	0.268	0.077	0.227	0.262	0.083	0.311	0.304	0.049	0.157	0.316	0.061	0.216
C4	0.306	0.054	0.196	0.300	0.067	0.256	0.328	0.035	0.112	0.334	0.046	0.151
C5	0.350	0.061	0.211	0.341	0.073	0.284	0.335	0.038	0.125	0.344	0.057	0.196
C6	0.308	0.056	0.202	0.301	0.069	0.269	0.329	0.036	0.114	0.335	0.050	0.161
$\{(T_1, T_2, T_1^*, T_2^*)\} = \{(1.5, 2.0, 1.5, 2.0)\}$												
A1	0.256	0.119	0.390	0.243	0.218	0.366	0.298	0.086	0.320	0.326	0.097	0.371
A2	0.265	0.250	1.006	0.245	0.520	0.318	0.300	0.090	0.325	0.329	0.110	0.403
A3	0.263	0.219	0.804	0.325	0.275	0.318	0.305	0.088	0.322	0.333	0.103	0.392
A4	0.267	0.089	0.306	0.253	0.098	0.343	0.327	0.074	0.228	0.322	0.081	0.275
A5	0.403	0.103	0.366	0.407	0.105	0.377	0.331	0.084	0.315	0.329	0.092	0.316
A6	0.393	0.092	0.354	0.287	0.104	0.370	0.331	0.077	0.233	0.326	0.086	0.314
B1	0.286	0.081	0.273	0.245	0.088	0.330	0.308	0.059	0.188	0.339	0.071	0.253
B2	0.254	0.083	0.286	0.246	0.090	0.334	0.303	0.065	0.207	0.333	0.076	0.263
B3	0.257	0.083	0.300	0.247	0.095	0.338	0.306	0.070	0.225	0.337	0.077	0.269
B4	0.270	0.072	0.236	0.261	0.084	0.315	0.313	0.050	0.168	0.343	0.062	0.227
B5	0.339	0.080	0.260	0.326	0.086	0.323	0.328	0.054	0.173	0.355	0.065	0.234
B6	0.297	0.075	0.251	0.286	0.084	0.318	0.319	0.053	0.171	0.348	0.063	0.228
C1	0.249	0.061	0.215	0.244	0.076	0.285	0.303	0.040	0.124	0.314	0.059	0.199
C2	0.252	0.062	0.220	0.246	0.078	0.305	0.305	0.042	0.139	0.317	0.059	0.204
C3	0.261	0.065	0.225	0.253	0.082	0.310	0.310	0.045	0.145	0.321	0.061	0.211
C4	0.268	0.052	0.194	0.262	0.066	0.256	0.329	0.034	0.108	0.334	0.046	0.149
C5	0.312	0.060	0.204	0.304	0.073	0.277	0.330	0.037	0.119	0.339	0.057	0.192
C6	0.278	0.055	0.199	0.272	0.069	0.262	0.325	0.035	0.113	0.331	0.048	0.157

Table 7: Interval assessments of γ_1

Test	ACI				BCI (LF-based)		BCI (SF-based)	
	$\{(T_1, T_2, T_1^*, T_2^*)\} = \{(0.5, 1.0, 0.5, 1.0)\}$							
A1	0.707	0.934	0.633	0.935	0.478	0.945	0.457	0.948
A2	0.783	0.925	0.700	0.927	0.484	0.945	0.465	0.947
A3	0.756	0.928	0.669	0.931	0.479	0.946	0.460	0.947
A4	0.605	0.940	0.481	0.944	0.444	0.951	0.423	0.953
A5	0.692	0.935	0.596	0.939	0.464	0.948	0.444	0.950
A6	0.670	0.938	0.582	0.941	0.457	0.950	0.437	0.951
B1	0.510	0.950	0.418	0.952	0.393	0.957	0.392	0.957
B2	0.541	0.945	0.472	0.947	0.430	0.953	0.410	0.955
B3	0.526	0.947	0.452	0.948	0.414	0.954	0.395	0.957
B4	0.401	0.956	0.372	0.960	0.363	0.962	0.360	0.962
B5	0.424	0.955	0.388	0.957	0.381	0.961	0.363	0.962
B6	0.436	0.953	0.401	0.955	0.388	0.959	0.375	0.960
C1	0.389	0.961	0.342	0.961	0.333	0.967	0.314	0.969
C2	0.391	0.958	0.363	0.961	0.343	0.965	0.329	0.967
C3	0.393	0.959	0.359	0.961	0.356	0.964	0.341	0.965
C4	0.330	0.962	0.324	0.963	0.283	0.970	0.274	0.972
C5	0.347	0.961	0.330	0.963	0.312	0.969	0.289	0.971
C6	0.351	0.960	0.338	0.962	0.327	0.969	0.295	0.970
	$\{(T_1, T_2, T_1^*, T_2^*)\} = \{(1.5, 2.0, 1.5, 2.0)\}$							
A1	0.655	0.938	0.586	0.942	0.475	0.948	0.451	0.950
A2	0.719	0.935	0.647	0.936	0.482	0.947	0.461	0.948
A3	0.678	0.937	0.619	0.939	0.470	0.949	0.456	0.949
A4	0.537	0.947	0.447	0.954	0.433	0.954	0.415	0.955
A5	0.618	0.941	0.526	0.944	0.456	0.951	0.440	0.951
A6	0.587	0.943	0.512	0.946	0.440	0.952	0.428	0.953
B1	0.458	0.956	0.413	0.959	0.392	0.958	0.382	0.960
B2	0.486	0.953	0.432	0.956	0.418	0.957	0.398	0.958
B3	0.473	0.954	0.429	0.957	0.413	0.957	0.394	0.958
B4	0.380	0.964	0.370	0.965	0.360	0.963	0.337	0.967
B5	0.392	0.963	0.381	0.964	0.363	0.962	0.362	0.963
B6	0.405	0.962	0.388	0.962	0.378	0.960	0.371	0.962
C1	0.356	0.968	0.333	0.969	0.320	0.971	0.308	0.971
C2	0.383	0.965	0.347	0.967	0.334	0.969	0.314	0.970
C3	0.366	0.966	0.359	0.967	0.343	0.965	0.336	0.967
C4	0.329	0.971	0.311	0.972	0.255	0.975	0.231	0.976
C5	0.334	0.970	0.320	0.971	0.287	0.973	0.274	0.974

(Continued)

Table 7 **(continued)**

C6	0.345	0.969	0.329	0.970	0.309	0.972	0.286	0.972

Table 8: Interval assessments of γ_2

Test	ACI				BCI (LF-based)		BCI (SF-based)	
$\{(T_1, T_2, T_1^*, T_2^*)\} = \{(0.5, 1.0, 0.5, 1.0)\}$								
A1	1.510	0.867	1.181	0.868	0.437	0.921	0.354	0.924
A2	1.688	0.848	1.348	0.853	0.455	0.917	0.389	0.915
A3	1.642	0.853	1.285	0.861	0.444	0.920	0.365	0.921
A4	1.376	0.881	0.940	0.898	0.403	0.928	0.302	0.937
A5	1.453	0.873	0.971	0.892	0.429	0.923	0.346	0.926
A6	1.389	0.880	0.970	0.894	0.419	0.925	0.331	0.930
B1	1.103	0.893	0.766	0.921	0.293	0.950	0.268	0.946
B2	1.368	0.887	0.931	0.904	0.322	0.945	0.285	0.942
B3	1.253	0.890	0.863	0.912	0.318	0.946	0.273	0.945
B4	0.889	0.920	0.710	0.927	0.238	0.959	0.211	0.961
B5	1.096	0.909	0.763	0.924	0.275	0.952	0.237	0.954
B6	0.901	0.914	0.735	0.926	0.250	0.955	0.227	0.957
C1	0.699	0.930	0.631	0.932	0.174	0.967	0.120	0.969
C2	0.855	0.926	0.708	0.928	0.203	0.964	0.149	0.966
C3	0.753	0.929	0.680	0.931	0.195	0.966	0.130	0.968
C4	0.526	0.936	0.504	0.938	0.126	0.969	0.106	0.971
C5	0.661	0.930	0.625	0.932	0.139	0.968	0.118	0.969
C6	0.569	0.934	0.554	0.936	0.134	0.968	0.111	0.970
$\{(T_1, T_2, T_1^*, T_2^*)\} = \{(1.5, 2.0, 1.5, 2.0)\}$								
A1	1.416	0.849	1.098	0.883	0.434	0.918	0.350	0.924
A2	1.464	0.843	1.336	0.863	0.440	0.917	0.366	0.920
A3	1.431	0.847	1.203	0.870	0.437	0.918	0.357	0.922
A4	1.287	0.874	0.919	0.907	0.414	0.923	0.281	0.942
A5	1.379	0.863	0.945	0.903	0.431	0.919	0.345	0.925
A6	1.329	0.869	0.925	0.906	0.427	0.920	0.296	0.939
B1	1.102	0.895	0.784	0.912	0.279	0.952	0.267	0.946
B2	1.257	0.877	0.893	0.908	0.294	0.948	0.279	0.943
B3	1.139	0.891	0.827	0.910	0.289	0.950	0.268	0.946
B4	0.845	0.923	0.709	0.925	0.217	0.961	0.203	0.961
B5	1.023	0.905	0.736	0.914	0.247	0.956	0.230	0.956
B6	0.853	0.916	0.723	0.918	0.235	0.958	0.220	0.959
C1	0.671	0.932	0.627	0.933	0.166	0.972	0.119	0.967

(Continued)

Table 8 **(continued)**

C2	0.812	0.928	0.687	0.926	0.186	0.968	0.127	0.965
C3	0.723	0.931	0.639	0.930	0.184	0.968	0.124	0.966
C4	0.515	0.938	0.492	0.941	0.126	0.981	0.092	0.972
C5	0.638	0.933	0.609	0.935	0.136	0.979	0.106	0.970
C6	0.546	0.936	0.539	0.938	0.132	0.980	0.102	0.971

Table 9: Interval assessments of ϕ

Test	ACI				BCI (LF-based)		BCI (SF-based)	
	$\{(T_1, T_2, T_1^*, T_2^*)\} = \{(0.5, 1.0, 0.5, 1.0)\}$							
A1	0.722	0.915	0.519	0.918	0.525	0.932	0.480	0.935
A2	0.634	0.923	0.466	0.927	0.448	0.938	0.433	0.941
A3	0.672	0.918	0.486	0.923	0.466	0.934	0.453	0.938
A4	0.504	0.930	0.443	0.932	0.433	0.943	0.404	0.944
A5	0.431	0.937	0.401	0.941	0.391	0.948	0.384	0.950
A6	0.443	0.932	0.432	0.939	0.399	0.946	0.396	0.948
B1	0.404	0.938	0.394	0.945	0.377	0.952	0.347	0.956
B2	0.392	0.943	0.365	0.946	0.355	0.960	0.305	0.965
B3	0.403	0.941	0.375	0.945	0.361	0.956	0.325	0.961
B4	0.323	0.954	0.292	0.956	0.128	0.969	0.128	0.970
B5	0.297	0.956	0.285	0.959	0.116	0.972	0.106	0.976
B6	0.313	0.955	0.288	0.957	0.122	0.971	0.117	0.973
C1	0.292	0.958	0.270	0.960	0.112	0.973	0.101	0.977
C2	0.282	0.960	0.253	0.961	0.101	0.976	0.097	0.978
C3	0.291	0.959	0.265	0.960	0.102	0.975	0.100	0.977
C4	0.264	0.961	0.247	0.962	0.095	0.977	0.095	0.978
C5	0.239	0.962	0.238	0.963	0.078	0.979	0.077	0.980
C6	0.254	0.962	0.246	0.962	0.093	0.978	0.079	0.980
	$\{(T_1, T_2, T_1^*, T_2^*)\} = \{(1.5, 2.0, 1.5, 2.0)\}$							
A1	0.692	0.925	0.587	0.927	0.468	0.941	0.471	0.943
A2	0.571	0.932	0.452	0.933	0.435	0.947	0.418	0.948
A3	0.603	0.928	0.476	0.931	0.447	0.944	0.431	0.946
A4	0.467	0.934	0.435	0.935	0.420	0.946	0.398	0.948
A5	0.429	0.940	0.397	0.944	0.384	0.953	0.382	0.955
A6	0.432	0.935	0.419	0.942	0.398	0.952	0.393	0.954
B1	0.401	0.941	0.388	0.948	0.377	0.958	0.340	0.960
B2	0.367	0.946	0.356	0.950	0.342	0.967	0.302	0.969
B3	0.386	0.944	0.372	0.948	0.367	0.962	0.319	0.964

(Continued)

Table 9 **(continued)**

B4	0.313	0.958	0.292	0.959	0.128	0.972	0.117	0.974
B5	0.292	0.959	0.284	0.961	0.116	0.975	0.101	0.979
B6	0.293	0.958	0.288	0.961	0.120	0.974	0.110	0.976
C1	0.291	0.961	0.269	0.961	0.105	0.976	0.100	0.980
C2	0.276	0.962	0.245	0.963	0.099	0.979	0.089	0.981
C3	0.285	0.962	0.252	0.962	0.101	0.979	0.092	0.980
C4	0.242	0.962	0.241	0.963	0.095	0.979	0.083	0.981
C5	0.224	0.963	0.238	0.964	0.077	0.982	0.073	0.982
C6	0.234	0.962	0.240	0.963	0.082	0.980	0.076	0.981

Table 10: Interval assessments of $\mathcal{R}$

Test	ACI				BCI (LF-based)		BCI (SF-based)	
A1	0.278	0.957	0.303	0.955	0.119	0.976	0.143	0.975
A2	0.304	0.953	0.330	0.950	0.127	0.974	0.153	0.973
A3	0.290	0.955	0.312	0.952	0.122	0.975	0.149	0.974
A4	0.213	0.963	0.229	0.960	0.107	0.978	0.129	0.977
A5	0.265	0.959	0.280	0.957	0.115	0.976	0.139	0.975
A6	0.252	0.960	0.270	0.958	0.111	0.977	0.133	0.976
B1	0.198	0.969	0.204	0.967	0.101	0.979	0.119	0.977
B2	0.202	0.968	0.210	0.965	0.104	0.979	0.123	0.978
B3	0.212	0.963	0.228	0.961	0.106	0.978	0.125	0.977
B4	0.164	0.973	0.189	0.970	0.096	0.981	0.098	0.980
B5	0.194	0.969	0.203	0.967	0.101	0.979	0.118	0.978
B6	0.180	0.970	0.200	0.968	0.097	0.980	0.108	0.979
C1	0.156	0.974	0.183	0.972	0.080	0.982	0.089	0.981
C2	0.158	0.974	0.185	0.971	0.084	0.982	0.089	0.981
C3	0.163	0.973	0.186	0.971	0.088	0.982	0.095	0.981
C4	0.129	0.976	0.170	0.974	0.054	0.985	0.067	0.983
C5	0.150	0.975	0.180	0.973	0.069	0.984	0.076	0.982
C6	0.148	0.975	0.175	0.973	0.065	0.984	0.071	0.982
				$\{(T_1, T_2, T_1^*, T_2^*)\} = \{(1.5, 2.0, 1.5, 2.0)\}$				
A1	0.258	0.960	0.290	0.957	0.112	0.977	0.116	0.977
A2	0.291	0.955	0.315	0.953	0.121	0.976	0.125	0.976
A3	0.281	0.957	0.291	0.955	0.115	0.977	0.122	0.976
A4	0.209	0.965	0.223	0.963	0.092	0.980	0.108	0.979
A5	0.244	0.962	0.271	0.959	0.098	0.978	0.112	0.977
A6	0.244	0.963	0.256	0.960	0.093	0.979	0.109	0.978
B1	0.191	0.971	0.200	0.969	0.086	0.981	0.103	0.980

(Continued)

Table 10 (continued)

B2	0.199	0.970	0.204	0.968	0.087	0.981	0.104	0.980
B3	0.207	0.965	0.222	0.963	0.090	0.980	0.107	0.979
B4	0.162	0.975	0.183	0.973	0.077	0.983	0.096	0.982
B5	0.189	0.972	0.198	0.969	0.079	0.981	0.101	0.980
B6	0.177	0.973	0.194	0.970	0.079	0.983	0.099	0.981
C1	0.150	0.977	0.174	0.974	0.070	0.984	0.083	0.983
C2	0.155	0.976	0.180	0.974	0.073	0.984	0.086	0.983
C3	0.161	0.976	0.181	0.973	0.074	0.985	0.089	0.983
C4	0.121	0.979	0.160	0.976	0.051	0.987	0.067	0.986
C5	0.141	0.977	0.173	0.975	0.060	0.986	0.075	0.984
C6	0.135	0.978	0.172	0.975	0.056	0.987	0.069	0.984

6 Microdroplets Data Analysis

Microdroplets serve as vectors for the transmission of infectious pathogens, including those responsible for severe respiratory illnesses. Empirical evidence indicates that sneezing generates aerosolized particles approximately 10 micrometers in diameter, which remain suspended in the air. These aerosols can harbor viruses and other pathogenic microorganisms, facilitating airborne transmission upon inhalation by susceptible individuals. Consequently, minimizing contact with potentially contaminated surfaces, avoiding proximity to infected persons, and limiting exposure to environments with active infections are critical mitigation strategies. Furthermore, variations in ambient airflow velocity significantly influence the airborne persistence of microdroplets, thereby modulating transmission risk; see and Rothman et al. [33].

For this purpose, in this part, we investigate the lifetime distribution of microdroplets in the ambient environment, framed as an application of the stress-strength model. In the practical setup, airflow velocity serves as the stress variable (X), and the strength variable (Y) denotes the maximum aerodynamic load a droplet can withstand before fragmentation. This representation allows direct estimation of the stress–strength reliability $\mathcal{R}$, quantifying the likelihood of droplet failure under given airflow conditions. This dataset was originally presented by Asadi et al. [34] and later rediscussed by Nassar and Elshahhat [35]. We now analyze average particle diameters (measured in meters per second, m/s) observed under two stress conditions: 0.35 m/s (with $n = 15$) and 0.20 m/s (with $n^* = 19$); see Table 11.

To assess the adequacy of the W distribution for modeling the microdroplet datasets, we first obtain the MLEs of $\gamma_i,\ i = 1, 2$ and ϕ, along with their corresponding standard errors (Std.Ers). Moreover, for more investigation, the 95% ACI estimates through LF-based of $\gamma_i,\ i = 1, 2$ and ϕ are also calculated with their interval widths (IWs). These estimates are subsequently employed to compute the Kolmogorov-Smirnov (KS) statistic and its associated p-value; see Table 12. Given that the observed p-value substantially exceeds the conventional significance level of $\alpha = 5\%$, we conclude that the W distribution provides a satisfactory fit to the microdroplet datasets.

Table 11: Time-to-fall of microdroplets in air

Data at 0.35 m/s									
0.47	0.54	0.55	0.80	0.96	1.14	1.24	1.30	1.38	1.50
1.61	1.61	1.70	1.79	1.80					
Data at 0.20 m/s									
0.8	0.9	1.15	1.15	1.25	1.3	1.4	0.97	1.01	1.09
1.15	1.18	1.22	1.27	1.29	1.31	1.34	1.36	1.37	

Table 12: Fitting summary of W lifespan model from microdroplet datasets

Group	Par.	MLE (Std.Er)	ACI			KS (p-Value)
			Low.	Upp.	IW	
X	ϕ	3.1634 (0.6955)	1.8002	4.5266	2.7264	0.1463 (0.9051)
	γ_1	0.3656 (0.1451)	0.0813	0.6499	0.5686	
Y	ϕ	9.5116 (1.8168)	5.9508	13.072	7.1217	0.1034 (0.9872)
	γ_2	0.1178 (0.0626)	0.0005	0.2406	0.2401	

Using a comprehensive suite of graphical diagnostics, Fig. 1 presents the goodness-of-fit assessment for the proposed W lifetime model applied to the microdroplet datasets through six complementary visual tools:

1. Fitted density curves overlaid on empirical histograms of the microdroplet lifetimes, allowing direct visual comparison between observed and modeled distributions;
2. Fitted reliability (survival) curves, highlighting the agreement between empirical survival probabilities and the model's predicted reliability function;
3. Probability–probability (PP) plots, evaluating the concordance between the empirical and theoretical cumulative probabilities;
4. Quantile–quantile (QQ) plots, assessing how well the theoretical quantiles align with the observed data across the distributional range;
5. Scaled total time on test (TTT) transforms, which provide an exploratory view of the underlying hazard rate structure;
6. Contour plots of the log-likelihood function for the parameter space, used to examine identifiability and estimation stability.

Panels (a)–(d) of Fig. 1 collectively demonstrate that the proposed W lifetime model offers an excellent fit to both microdroplet datasets across multiple diagnostic perspectives. In particular, the high degree of alignment in the PP and QQ plots, together with the close adherence of fitted curves to empirical trends, confirm the model's adequacy. Furthermore, the scaled TTT plots in Fig. 1e reveal a consistently increasing failure rate in both datasets—an expected and practically relevant hazard pattern frequently associated with the W distribution family. Finally, the contour diagram in Fig. 1f shows well-defined and unimodal likelihood surfaces for the MLEs of γ_i, $i = 1, 2$ and ϕ, ensuring their existence and uniqueness. This property supports the use of these MLEs as reliable initial values for all subsequent estimation and optimization procedures.

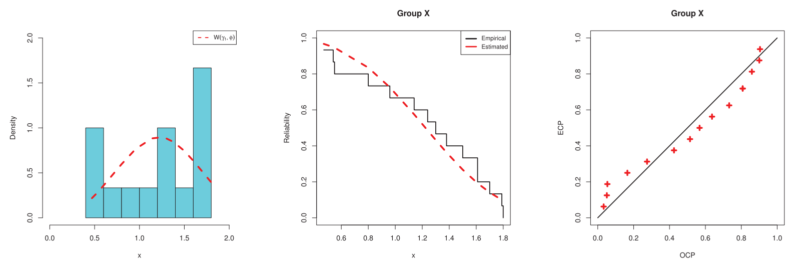

(a) PDF (b) RF (c) PP

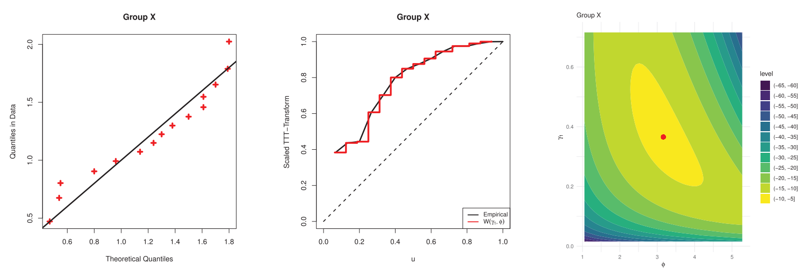

(d) QQ (e) TTT (f) Contour

(i) Group-X

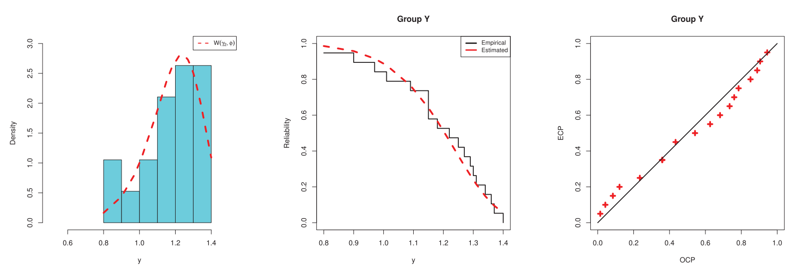

(a) PDF (b) RF (c) PP

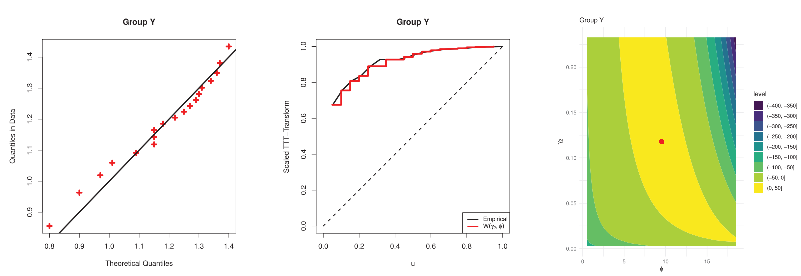

(d) QQ (e) TTT (f) Contour

(ii) Group-Y

Figure 1: Visualization diagrams of the W lifespan model from microdroplet datasets (**a–f**)

To examine the acquired point and interval estimators of γ_i, $i = 1, 2$, ϕ, and $\mathcal{R}$, for each group of microdroplet datasets listed in Table 11, four artificial UTIPHC samples (denoted by $\mathbb{S}[i]$, for $i = 1, 2, 3$) based on $k = k^* = 5$, $r = r^* = 10$, $\mathbf{R} = (1^{\star}5, 2^{\star}5)$, $S^* = (1^{\star}9, 0^{\star}1)$, and varying selections of T_i and T_i^* $(i = 1, 2)$ are created; see Table 13. For each sample listed in Table 13, the point estimates (along with their Std.Ers) and 95% interval estimates (along with their IWs) of γ_i, $i = 1, 2$, ϕ, and $\mathcal{R}$ are computed using the proposed frequentist and Bayes methodologies; see Table 14. Given the absence of informative prior knowledge regarding the W parameters from the microdroplet datasets, all Bayesian analyses are performed using a joint improper gamma prior. Without loss of generality, we set $\mathcal{M} = 50{,}000$ with a burn-in period of size 10,000 iterations to obtain all Bayesian point and credible inferences for γ_i, $i = 1, 2$, ϕ, and $\mathcal{R}$. The initial values for the MCMC chains are chosen based on the fitted frequentist estimates (provided in Table 14) of γ_i, $i = 1, 2$, and ϕ developed by ML and MPS approaches. It is observed from Table 14 that the MCMC-based estimates for γ_i, $i = 1, 2$, ϕ, or $\mathcal{R}$ exhibit desirable performance, yielding the smallest standard error estimates compared to all frequentist counterparts. A similar pattern is observed when comparing the BCI estimates (through LF-based and SF-based) to their competitive ACI estimates (through LF-based and SF-based) in terms of shortest IWs.

Table 13: Artificial UTIPHC samples from microdroplet datasets

Sample	$T_1(d_1)$ $T_1^*(d_1^*)$	$T_2(d_2)$ $T_2^*(d_2^*)$	R^* S^*	(T, T^*)	Data
$\mathbb{S}[1]$	1.75(10)	1.80(10)	0	(1.70, 1.34)	0.47, 0.54, 0.80, 0.96, 1.24, 1.30, 1.50, 1.61, 1.61, 1.70
	1.35(10)	1.40(10)	0		0.80, 0.97, 1.01, 1.09, 1.15, 1.22, 1.25, 1.27, 1.29, 1.34
$\mathbb{S}[2]$	1.65(8)	1.70(8)	2	(1.65, 1.40)	0.47, 0.80, 1.14, 1.24, 1.30, 1.38, 1.50, 1.61
	1.40(8)	1.45(8)	3		0.80, 1.01, 1.09, 1.18, 1.22, 1.27, 1.31, 1.36
$\mathbb{S}[3]$	0.85(3)	1.35(5)	5	(1.30, 1.22)	0.47, 0.55, 0.80, 1.14, 1.30
	0.99(2)	1.25(5)	9		0.80, 0.97, 1.01, 1.15, 1.22
$\mathbb{S}[4]$	0.55(1)	1.25(4)	7	(1.25, 1.30)	0.47, 0.80, 1.14, 1.24
	0.85(1)	1.30(4)	11		0.80, 1.01, 1.15, 1.27

Table 14: Estimates of $\gamma_i,\ i=1,2,\ \phi$, and $\mathcal{R}$ from microdroplet datasets

Sample	Par.	MLE / MPSE		MCMC LF-based / MCMC SF-based		95% ACI-LF / 95% ACI-SF			95% BCI-LF / 95% BCI-SF		
		Est.	Std.Er	Est.	Std.Er	Low.	Upp.	IW	Low.	Upp.	IW
$\mathbb{S}[1]$	γ_1	4.3131	0.9145	4.2970	0.0428	2.5207	6.1055	3.5848	4.2195	4.3749	0.1554
		4.9975	1.5392	4.9850	0.0370	1.9807	8.0143	6.0336	4.9172	5.0529	0.1357
	γ_2	7.4014	1.6526	7.3858	0.0426	4.1625	10.640	6.4779	7.3101	7.4644	0.1543
		8.3251	2.2619	8.3131	0.0371	3.8919	12.758	8.8665	8.2433	8.3810	0.1378
	ϕ	0.1846	0.0692	0.1750	0.0296	0.0489	0.3202	0.2713	0.1232	0.2319	0.1087
		0.1472	0.0779	0.1400	0.0249	0.0056	0.2943	0.3055	0.0954	0.1891	0.0938
	$\mathcal{R}$	0.3682	0.0525	0.3678	0.0025	0.2652	0.4712	0.2060	0.3628	0.3726	0.0098
		0.3751	0.0558	0.3749	0.0019	0.2658	0.4845	0.2187	0.3712	0.3786	0.0075
$\mathbb{S}[2]$	γ_1	4.5303	1.0888	4.5262	0.0204	2.3963	6.6644	4.2681	4.4871	4.5653	0.0783
		5.4496	1.3539	5.4457	0.0204	2.7961	8.1032	5.3071	5.4069	5.4848	0.0779
	γ_2	6.0803	1.5196	6.0761	0.0204	3.1018	9.0587	5.9569	6.0372	6.1152	0.0781
		6.9915	1.9112	6.9874	0.0204	3.2457	10.737	7.4916	6.9482	7.0267	0.0785
	ϕ	0.1247	0.0534	0.1205	0.0172	0.0201	0.2293	0.2092	0.0885	0.1544	0.0659
		0.0873	0.0465	0.0838	0.0153	0.0039	0.1785	0.1746	0.0558	0.1139	0.0581
	$\mathcal{R}$	0.4270	0.0608	0.4269	0.0013	0.3078	0.5462	0.2384	0.4242	0.4295	0.0053
		0.4380	0.0581	0.4380	0.0011	0.3242	0.5518	0.2276	0.4358	0.4403	0.0045
$\mathbb{S}[3]$	γ_1	2.7785	1.0943	2.7742	0.0205	0.6337	4.9232	4.2895	2.7350	2.8135	0.0784
		2.9461	1.3061	2.9421	0.0204	0.3862	5.5060	5.1198	2.9030	2.9810	0.0780
	γ_2	4.9883	1.8245	4.9842	0.0204	1.4123	8.5644	7.1521	4.9453	5.0235	0.0782
		5.2360	2.1448	5.2319	0.0204	1.0323	9.4398	8.4075	5.1928	5.2710	0.0782
	ϕ	0.1747	0.0673	0.1695	0.0196	0.0428	0.3065	0.2637	0.1329	0.2070	0.0741
		0.1411	0.0624	0.1356	0.0193	0.0188	0.2634	0.2445	0.0997	0.1722	0.0726
	$\mathcal{R}$	0.3577	0.1150	0.3576	0.0019	0.1323	0.5832	0.4509	0.3539	0.3612	0.0074
		0.3601	0.1274	0.3599	0.0018	0.1103	0.6099	0.4996	0.3564	0.3634	0.0070
$\mathbb{S}[4]$	γ_1	3.4483	1.5303	3.4440	0.0205	0.4490	6.4475	5.9985	3.4047	3.4834	0.0786
		4.5379	2.3508	4.5340	0.0204	0.0095	9.1453	9.1358	4.4951	4.5731	0.0780
	γ_2	3.9635	1.6339	3.9593	0.0204	0.7611	7.1658	6.4047	3.9203	3.9985	0.0782
		4.4013	2.0838	4.3971	0.0204	0.3172	8.4854	8.1682	4.3580	4.4364	0.0784
	ϕ	0.1209	0.0543	0.1156	0.0188	0.0145	0.2272	0.2127	0.0806	0.1518	0.0712
		0.0820	0.0461	0.0768	0.0177	0.0008	0.1723	0.1715	0.0450	0.1108	0.0658
	$\mathcal{R}$	0.4652	0.1366	0.4652	0.0019	0.1976	0.7329	0.5354	0.4614	0.4689	0.0075
		0.5076	0.1508	0.5077	0.0016	0.2121	0.8032	0.5911	0.5046	0.5108	0.0062

To examine the existence and uniqueness of the MLEs and MPSEs of $\gamma_i,\ i = 1,2$, and ϕ, Figs. 2 and 3 present the contour plots using log-LF and log-SF, respectively, derived from samples $\mathbb{S}[i]$ for $i = 1,2,3,4$. These contours indicate that the frequentist (MLE/MPSE) estimates obtained from microdroplet datasets exist and are also unique. These visual results are consistent with the numerical estimates reported in Table 14. Furthermore, using $\mathbb{S}[1]$ as a representative case, Fig. 4 displays Gaussian kernel density estimates and trace plots for $\gamma_i,\ i = 1,2$, ϕ, and $\mathcal{R}$. Fig. 4, using the first 40,000 MCMC posterior iterations of $\gamma_i,\ i = 1,2$, ϕ, and $\mathcal{R}$, reveals an adequate mixing behavior. It also confirms that the length of the burned-in period is sufficient to eliminate early transients and achieve convergence. Lastly, Fig. 4 also reveals distributional characteristics of the marginal posterior estimates of $\gamma_i,\ i = 1,2$, ϕ, or $\mathcal{R}$ appear approximately symmetric.

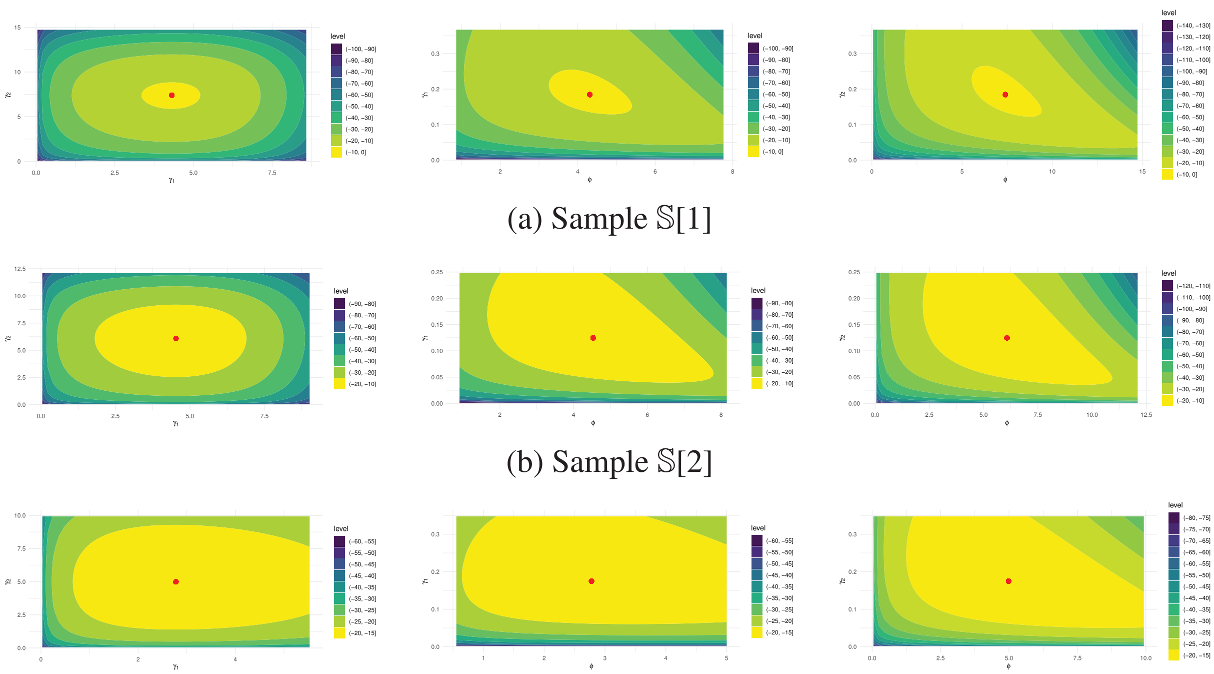

(a) Sample $\mathbb{S}[1]$

(b) Sample $\mathbb{S}[2]$

(c) Sample $\mathbb{S}[3]$

(i) (γ_1, γ_2) (ii) (ϕ, γ_1) (iii) (ϕ, γ_2)

Figure 2: Contours from log-LF for $\gamma_i,\ i = 1,2$, and ϕ from microdroplet datasets (**a–c**)

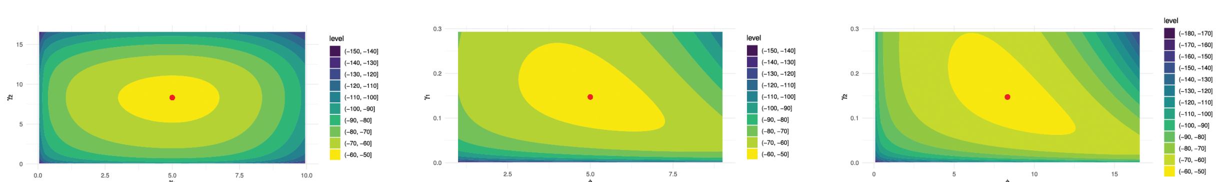

(a) Sample $\mathbb{S}[1]$

Figure 3: (Continued)

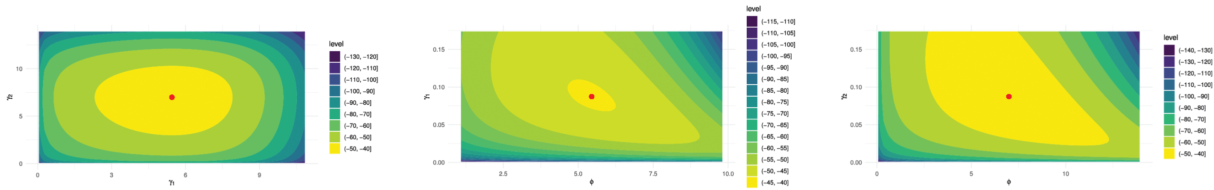

(b) Sample $\mathbb{S}[2]$

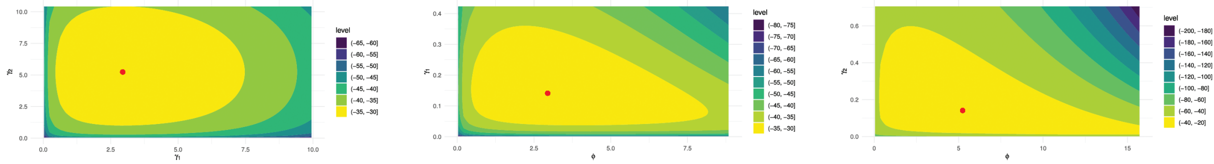

(c) Sample $\mathbb{S}[3]$

(i) (γ_1, γ_2) (ii) (ϕ, γ_1) (iii) (ϕ, γ_2)

Figure 3: Contours from log-SF for $\gamma_i,\ i = 1, 2$, and ϕ from microdroplet datasets (**a–c**)

In summary, based on the analysis of both microdroplet datasets, it can be concluded that the Weibull lifetime model provides a more appropriate framework for evaluating reliability characteristics when the lifetimes are observed under the proposed UTIPHC scheme.

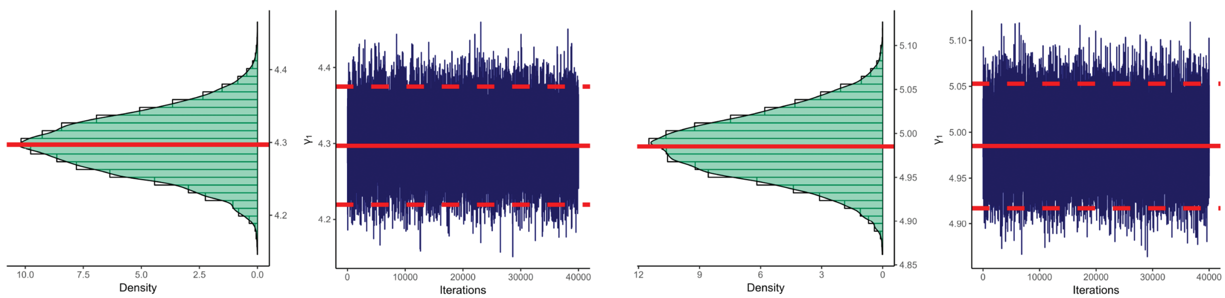

(a) Trace/Density plots of γ_1

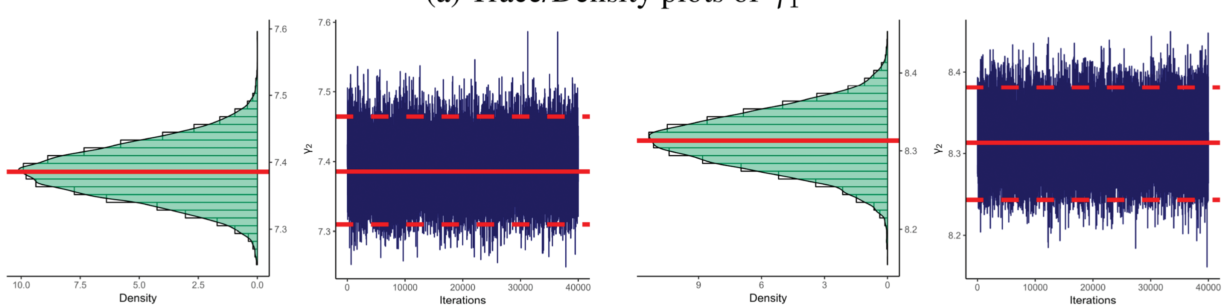

(b) Trace/Density plots of γ_2

Figure 4: (Continued)

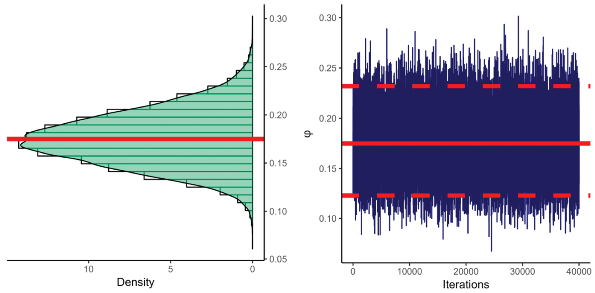

(c) Trace/Density plots of ϕ

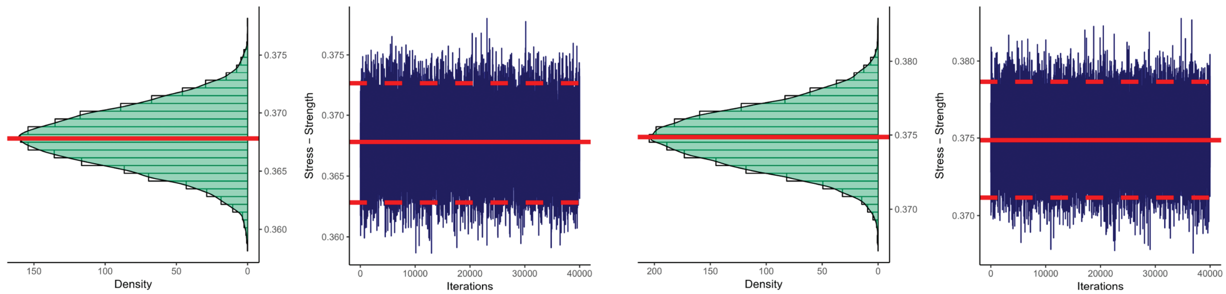

(d) Trace/Density plots of $\mathcal{R}$

(i) MCMC (LF-based) (ii) MCMC (SF-based)

Figure 4: The MCMC diagrams of $\gamma_i,\ i = 1, 2$, and ϕ from microdroplet datasets (**a–d**)

7 Concluding Remarks

In this study, we addressed the estimation of the stress-strength reliability parameter $\phi = P(Y < X)$ under the unified Type-I progressively hybrid censoring scheme, assuming independent Weibull-distributed stress and strength variables. By deriving the maximum likelihood and maximum product of spacings estimators, along with their corresponding interval estimates, and investigating Bayesian estimation through both likelihood- and spacing-based approaches, we advance the methodological tools for reliability analysis under complex censoring. This work makes three key contributions: (1) We developed a comprehensive framework that integrates theoretical results and simulation studies to facilitate the practical implementation of the unified Type-I progressively hybrid censoring scheme. (2) We introduced and assessed non-likelihood-based estimation methods, such as maximum product of spacings estimation and Bayesian approaches using spacing-based posteriors. These methods were shown to be effective alternatives, especially in situations where traditional likelihood-based methods may perform poorly. (3) We demonstrated the practical value of the stress-strength parameter under the unified Type-I progressively hybrid censoring scheme using real-world data. Overall, our simulation results and real-data findings demonstrate that the proposed estimation procedures are both reliable and accurate, supporting the potential use of the unified Type-I progressively hybrid censoring scheme in modern reliability analysis.

Acknowledgement: The authors express their gratitude to Princess Nourah bint Abdulrahman University Researchers Supporting Project number (PNURSP2025R50), Princess Nourah bint Abdulrahman University, Riyadh, Saudi Arabia.

Funding Statement: This research was funded by Princess Nourah bint Abdulrahman University Researchers Supporting Project number (PNURSP2025R50), Princess Nourah bint Abdulrahman University, Riyadh, Saudi Arabia.

Author Contributions: The authors confirm contribution to the paper as follows: study conception and design: Mazen Nassar, Refah Alotaibi, Ahmed Elshahhat; data collection: Refah Alotaibi; analysis and interpretation of results: Ahmed Elshahhat; draft manuscript preparation: Mazen Nassar, Ahmed Elshahhat. All authors reviewed the results and approved the final version of the manuscript.

Availability of Data and Materials: The data that support the findings of this study are available within the paper.

Ethics Approval: Not applicable.

Conflicts of Interest: The authors declare no conflicts of interest to report regarding the present study.

References

1. Liu X, Yu X, Tong J, Wang X, Wang X. Mixed uncertainty analysis for dynamic reliability of mechanical structures considering residual strength. Reliab Eng Syst Saf. 2021;209(6):107472. doi:10.1016/j.ress.2021.107472.
2. Cheng T, Fan D, Liu X, Wang J. Reliability analysis for manufacturing system of drive shaft based on dynamic Bayesian network. Qual Reliab Eng Int. 2024;40(8):4482–97. doi:10.1002/qre.3644.
3. Kotb MS, Raqab MZ. Inferential analysis of the stress-strength reliability for a new extended family of distributions. Res Statist. 2025;3(1):2452926. doi:10.1080/27684520.2025.2452926.
4. Birnbaum ZW, McCarty RC. A distribution-free upper confidence bound for Pr $\{Y < X\}$, based on independent samples of X and Y. Ann Math Stat. 1958;29(2):558–62. doi:10.1214/aoms/1177706631.
5. Asgharzadeh A, Valiollahi R, Raqab MZ. Stress-strength reliability of Weibull distribution based on progressively censored samples. SORT-Stat Oper Res Trans. 2011;35(2):103–24.
6. Asgharzadeh A, Valiollahi R, Raqab MZ. Estimation of the stress-strength reliability for the generalized logistic distribution. Stat Methodol. 2013;15(2):73–94. doi:10.1016/j.stamet.2013.05.002.
7. Krishna H, Dube M, Garg R. Estimation of stress strength reliability of inverse Weibull distribution under progressive first failure censoring. Aust J Stat. 2019;48(1):14–37. doi:10.17713/ajs.v47i4.638.
8. Almarashi AM, Algarni A, Nassar M. On estimation procedures of stress-strength reliability for Weibull distribution with application. PLoS One. 2020;15(8):e0237997. doi:10.1371/journal.pone.0237997.
9. Kotb MS, Al Omari MA. Estimation of the stress-strength reliability for the exponential-Rayleigh distribution. Math Comput Simulat. 2025;228(3):263–73. doi:10.1016/j.matcom.2024.09.005.
10. Lai CD, Murthy DNP, Xie M. Weibull distributions. WIREs Comput Stat. 2011;3(3):282–7. doi:10.1002/wics.157.
11. Epstein B. Truncated life tests in the exponential case. Ann Math Stat. 1954;25(3):555–64. doi:10.1214/aoms/1177728723.
12. Childs A, Chandrasekar B, Balakrishnan N, Kundu D. Exact likelihood inference based on Type-I and Type-II hybrid censored samples from the exponential distribution. Ann Inst Stat Math. 2003;55(2):319–30. doi:10.1007/bf02530502.
13. Balakrishnan N, Kundu D. Hybrid censoring: models, inferential results and applications. Comput Stat Data Anal. 2013;57(1):166–209.

14. Chandrasekar B, Childs A, Balakrishnan N. Exact likelihood inference for the exponential distribution under generalized Type-I and Type-II hybrid censoring. Nav Res Logist. 2004;51(7):994–1004. doi:10.1002/nav.20038.
15. Balakrishnan N, Rasouli A, Sanjari Farsipour N. Exact likelihood inference based on an unified hybrid censored sample from the exponential distribution. J Stat Comput Simul. 2008;78(5):475–88. doi:10.1080/00949650601158336.
16. Panahi H, Sayyareh A. Estimation and prediction for a unified hybrid-censored Burr Type XII distribution. J Stat Comput Simul. 2016;86(1):55–73. doi:10.1080/00949655.2014.993985.
17. Jeon YE, Kang SB. Estimation of the Rayleigh distribution under unified hybrid censoring. Aust J Stat. 2021;50(1):59–73. doi:10.17713/ajs.v50i1.990.
18. Alotaibi R, Nassar M, Khan ZA, Alajlan WA, Elshahhat A. Entropy evaluation in inverse Weibull unified hybrid censored data with application to mechanical components and head-neck cancer patients. AIMS Math. 2025;10(1):1085–115. doi:10.3934/math.2025052.
19. Górny J, Cramer E. Modularization of hybrid censoring schemes and its application to unified progressive hybrid censoring. Metrika. 2018;81(2):173–210. doi:10.1007/s00184-017-0639-7.
20. Anwar S, Lone SA, Khan A, Almutlak S. Stress-strength reliability estimation for the inverted exponentiated Rayleigh distribution under unified progressive hybrid censoring with application. Electr Res Arch. 2023;31(7):4011–33. doi:10.3934/era.2023204.
21. Lone SA, Panahi H, Anwar S, Shahab S. Estimations and optimal censoring schemes for the unified progressive hybrid gamma-mixed Rayleigh distribution. Elect Res Arch. 2023;31(8):4729–52. doi:10.3934/era.2023242.
22. Dutta S, Ng HKT, Kayal S. Inference for Kumaraswamy-G family of distributions under unified progressive hybrid censoring with partially observed competing risks data. Stat Neerl. 2024;78(4):719–42. doi:10.1111/stan.12357.
23. Dutta S, Kayal S. Estimation and prediction for Burr type III distribution based on unified progressive hybrid censoring scheme. J Appl Stat. 2024;51(1):1–33. doi:10.1080/02664763.2022.2113865.
24. Bayoud HA, Almathkour FB, Raqab MZ. Advanced inference techniques for two-parameter Topp-Leone models under unified progressively hybrid censoring. Commun Stat Simul Comput. 2024. doi:10.1080/03610918.2024.2440620.
25. Cheng RCH, Amin NAK. Estimating parameters in continuous univariate distributions with a shifted origin. J R Stat Soc Series B Stat Methodol. 1983;45(3):394–403. doi:10.1111/j.2517-6161.1983.tb01268.x.
26. Ranneby B. The maximum spacing method. An estimation method related to the maximum likelihood method. Scand J Stat. 1984;11(2):93–112.
27. Kateri M, Nikolov NI. Product of spacings estimation in step-stress accelerated life testing: an alternative to maximum likelihood. IEEE Trans Reliab. 2024;73(3):1433–45. doi:10.1109/tr.2024.3369977.
28. Nassar M, Alotaibi R, Elshahhat A. E-bayesian estimation using spacing function for inverse lindley adaptive type-I progressively censored samples: comparative study with applications. Appl Bionics Biomech. 2024;2024(1):5567457. doi:10.1155/2024/5567457.
29. Nassar M, Elshahhat A. Estimation procedures and optimal censoring schemes for an improved adaptive progressively type-II censored Weibull distribution. J Appl Stat. 2024;51(9):1664–88. doi:10.1080/02664763.2023.2230536.
30. R Core Team. *R: a language and environment for statistical computing*, Vienna, Austria: R Foundation for Statistical Computing; 2022 [Internet]. [cited 2025 Sep 1]. Available from: https://www.R-project.org/.
31. Henningsen A, Toomet O. maxLik: a package for maximum likelihood estimation in R. Comput Stat. 2011;26(3):443–58. doi:10.1007/s00180-010-0217-1.
32. Plummer M, Best N, Cowles K, Vines K. CODA: convergence diagnosis and output analysis for MCMC. R News. 2006;6:7–11.

33. Rothman KJ, Huybrechts KF, Murray EJ. Epidemiology: an introduction. 3rd ed. Oxford, UK: Oxford University Press; 2024.
34. Asadi S, Panahi H, Swarup C, Lone SA. Inference on adaptive progressive hybrid censored accelerated life test for Gompertz distribution and its evaluation for virus-containing micro droplets data. Alex Eng J. 2022;61(12):10071–84. doi:10.1016/j.aej.2022.02.061.
35. Nassar M, Elshahhat A. Statistical analysis of inverse Weibull constant-stress partially accelerated life tests with adaptive progressively type I censored data. Mathematics. 2023;11(2):370. doi:10.3390/math11020370.